

1
2
3
4
5
6
7
8
9
10
11
12
13
14
15
16
17
18
19
20
21
22
23
24
25
26
27
28
29
30
31

**GPR17 is an Essential Regulator for the Temporal Adaptation of Sonic Hedgehog
Signalling in Neural Tube Development**

**Atsuki Yatsuzuka¹, Akiko Hori¹, Minori Kadoya¹, Mami Matsuo-Takasaki^{2,4},
Toru Kondo³ and Noriaki Sasai^{1*}**

1. Developmental Biomedical Science, Graduate School of Biological Sciences, Nara Institute of Science and Technology, 8916-5, Takayama-cho, Ikoma 630-0192, Japan
2. Department of Regenerative Medicine and Stem Cell Biology, Faculty of Medicine, University of Tsukuba, Tsukuba 305-8575, Japan
3. Division of Stem Cell Biology, Institute for Genetic Medicine, Hokkaido University, Kita-15, Nishi-7, Kita-Ku, Sapporo 060-0815, Japan
4. Present Address: iPS Cell Advanced Characterization and Development Team, RIKEN BioResource Research Center, 3-1-1 Koyadai, Tsukuba, Ibaraki 305-0074, Japan

* Correspondence to Noriaki Sasai
E-mail: noriakisasai@bs.naist.jp
Tel: +81-743-72-5650

32 **Abstract**

33 Dorsal-ventral pattern formation of the neural tube is regulated by temporal and spatial activities of
34 extracellular signalling molecules. Sonic hedgehog (Shh) assigns ventral neural subtypes via activation
35 of the Gli transcription factors. Shh activity in the neural progenitor cells changes dynamically during
36 differentiation, but the mechanisms regulating this dynamicity are not fully understood.

37 Here we show that temporal change of the intracellular cAMP level confers the temporal Shh signal,
38 and the purinergic-type G-protein coupled receptor GPR17 plays an essential role for this regulation.
39 GPR17 is highly expressed in the ventral progenitor regions of the neural tube and acts as a negative
40 regulator of the Shh signal in chick embryos. While the activation of the GPR17-related signal inhibits
41 ventral identity, perturbation of *GPR17* expression leads to aberrant expansion of ventral neural domains.
42 Notably, perturbation of *GPR17* expression partially inhibits the negative feedback of Gli activity.
43 Moreover, GPR17 increases cAMP activity, suggesting that it exerts its function by inhibiting the
44 processing of Gli3 protein. GPR17 also negatively regulates Shh signalling in neural cells differentiated
45 from mouse embryonic stem cells, suggesting that GPR17 function is conserved among different
46 organisms. Our results demonstrate that GPR17 is a novel negative regulator of Shh signalling in a wide
47 range of cellular contexts.

48 **Introduction**

49 The neural tube, the embryonic organ of the central nervous system, consists of neural
50 progenitors and post-mitotic neurons arrayed in an orderly manner (Le Dreau and Marti, 2012; Ribes
51 and Briscoe, 2009). During neural tube development, extracellular signalling molecules (“morphogens”)
52 produced in the signalling centres of the organ provide positional cues to uncommitted neural progenitor
53 cells, and thereby assign the cellular fates in a concentration-dependent manner (Dessaud et al., 2008).
54 Identifying the molecular mechanism by which cells convert positional information into fate
55 determination is one of the major goals of developmental biology.(Dessaud et al., 2008)

56 Sonic hedgehog (Shh) is a signalling molecule expressed in the floor plate (FP) of the neural
57 tube and its underlying mesodermal tissue, the notochord. Shh plays essential roles in the assignment of
58 ventral identities (Dessaud et al., 2008). At the cellular level, the Shh ligand binds to the 12-span
59 transmembrane protein Patched 1 (Ptch1) at the primary cilia. The binding activates another membrane
60 protein, Smoothened (Smo). Smo further activates the transcription factors Gli2/3, which are transported
61 into the nucleus to induce the expression of their target genes (Dessaud et al., 2008). Gli2 and Gli3 have
62 dual activities; in the absence of Shh, the precursor Gli2/3 proteins associate with the scaffold protein
63 SuFu to form complexes with Cullin3 and Protein Kinase A (PKA), and are phosphorylated and
64 proteolytically processed into their repressor forms (Niewiadowski et al., 2014; Tempe et al., 2006;
65 Tuson et al., 2011; Wang and Li, 2006). In response to the Shh ligand, these complexes are dissociated,
66 ubiquitination is perturbed, and Gli2/3 are converted into their active forms (Niewiadowski et al., 2014;
67 Pan et al., 2006; Wang et al., 2000).

68 In the spinal cord, Shh forms a ventral-to-dorsal gradient with the highest level in the FP, and
69 is required for the assignment of at least five ventral neural progenitor domains in addition to FP
70 (Dessaud et al., 2008; Ribes and Briscoe, 2009). The ventral domains include p0-p2, pMN, p3 that are
71 arrayed in this order from dorsal to ventral, and can be defined by transcription factors expressed in a
72 domain-specific manner. For instance, two transcription factors Olig2 and Nkx2.2 are expressed in the
73 pMN and p3 domains, respectively, and are essential for these identities (Briscoe et al., 1999; Holz et
74 al., 2010; Lu et al., 2000). During the neural tube development, Olig2 responds to Shh and is expressed
75 first, and the expression of Nkx2.2, which is also a responsive gene to Shh, expression begins later
76 (Dessaud et al., 2007). The higher concentration of Shh allows the quicker switch from Olig2- to
77 Nkx2.2-expressing state in the progenitor cells (Dessaud et al., 2010). In this manner, the progenitor
78 cells exposed to a higher Shh concentration form the Nkx2.2-positive p3 domain at a more ventral
79 position than the Olig2/pMN domain. Thus, the Shh gradient is reflected in the dynamic expression of
80 the transcription factors, and a various cell types are formed in the spinal cord (Balaskas et al., 2012).

81 The Gli activity partially reflects the concentration of Shh at the initial step of neural
82 differentiation (Dessaud et al., 2010). After it is initially elevated, however, Gli activity decreases over
83 time (Balaskas et al., 2012; Dessaud et al., 2010). Moreover, the half-life of the signal intensity
84 determines the kinetics of the conversion of the downstream transcription factors that characterise the
85 neural domains. Therefore, the dynamic change of Gli activity, which is termed temporal adaptation, is

86 important for correct pattern formation of the neural tube (Balaskas et al., 2012; Dessaud et al., 2010;
87 Dessaud et al., 2007; Stamatakis et al., 2005).

88 Multiple mechanisms have been proposed to explain this adaptation (Cohen et al., 2015). One
89 model involves upregulation of the *Ptch1* gene. Since *Ptch1* is a negative regulator of the Shh signal,
90 accumulation of *Ptch1* depletes Shh and consequently decreases its intracellular signalling activity
91 (Dessaud et al., 2007). In addition, the expression level of the transcription factor *Gli2* decreases over
92 time, and the transduction of the Shh signal is thus reduced as the neural development proceeds (Cohen
93 et al., 2015). Importantly, this adaptation takes place only in the context of the neural differentiation,
94 and not in cultured cells, such as NIH3T3 fibroblast cells (Cohen et al., 2015; Humke et al., 2010; Ribes
95 and Briscoe, 2009), suggesting that some key genes are specifically induced in a developmental context.
96 However, such regulators have yet to be identified.

97 In parallel with Shh activity, intracellular cyclic AMP (cAMP) level and the activity of the
98 downstream mediator PKA have critical roles for the neural tube pattern formation (Epstein et al., 1996;
99 Tuson et al., 2011). Absence of PKA activity affects the subcellular localisation and processing of Gli
100 proteins at the cellular level, and results in the expansion of the ventral domains of the neural tube
101 (Tuson et al., 2011). Likewise, the activity of adenylyl cyclase 5 and 6 (AC5 and AC6, respectively),
102 which encourage the production of cAMP by resolving adenosine triphosphate (ATP), affects the Gli
103 activity and determination of the ventral cell fate (Moore et al., 2016; Vuolo et al., 2015). Moreover, G-
104 protein coupled receptors (GPCRs) have been suggested to control the neural tube pattern formation
105 through regulating the intracellular cAMP level (Humke et al., 2010; Pusapati et al., 2018). GPCRs
106 couple with G-proteins that are comprised of $G\alpha$, $G\beta$ and $G\gamma$ subunits. G-proteins are categorised into
107 several subclasses based on the type of the $G\alpha$ protein; $G\alpha_s$ and $G\alpha_q$ can potentiate the cAMP level,
108 whereas $G\alpha_i$ decreases this level (Rosenbaum et al., 2009). With respect to the neural tube development
109 and Shh signal, GPR161 has been suggested to interact with $G\alpha_s$ and negatively regulates the ventral
110 neural identities by elevating the cAMP level (Mukhopadhyay et al., 2013). Conversely, GPR175
111 interacts with $G\alpha_i$ protein and enhances the Shh signal (Singh et al., 2015). Therefore, the
112 GPCR/cAMP/PKA axis is a critical regulatory pathway in the neural tube pattern formation. However,
113 the molecular mechanisms by which cAMP level and PKA activity are involved in the temporal changes
114 of Gli activity remain to be revealed.

115 In this study, we found that the PKA activity changes over time in the ventral neural progenitor
116 cells, and thus hypothesised the existence of the regulatory molecule(s) for this change. As cAMP/PKA
117 level is often regulated by GPCRs, we searched for the GPCRs induced by Shh, and performed a
118 quantitative RT-PCR (RT-qPCR)-based screen in chick neural explants. We consequently identified
119 *GPR17* as a candidate gene. *GPR17* is induced by Shh, but negatively regulates the Shh signal. *GPR17*
120 also functions as a negative regulator in neural differentiation of mouse embryonic stem (ES) cells.
121 Taken together, our findings demonstrate that *GPR17* is a negative regulator of Shh signal in multiple
122 cellular contexts.

123 **Results**

124 **Temporal change of PKA activity confers temporal adaptation of the Shh signal**

125 For understanding the mechanisms by which the temporal adaptation (Cohen et al., 2015;
126 Dessaud et al., 2010; Dessaud et al., 2007) against the Shh signal takes place in the neural progenitor
127 cells, we reasoned that the PKA activity changes over time (Epstein et al., 1996; Tuson et al., 2011;
128 Vuolo et al., 2015). To address this hypothesis, we performed an *ex vivo* analysis using chick
129 intermediate neural explants. We isolated neural progenitor cells from the preneural tube area (Delfino-
130 Machin et al., 2005) of HH stage 9 (Hamburger and Hamilton, 1992) chick embryos and cultured the
131 cells for 24 hours. In the explants cultured with the low Shh concentration (Shh^L; see Fig. S1B-H and
132 Materials and Methods), the majority of the cells expressed Olig2 with a small subset of Nkx2.2-positive
133 cells (Fig. 1A,C,E,G). However, in the explants cultured with the PKA inhibitor H-89 together with
134 Shh^L, the Nkx2.2-positive cells dominated the explants (Fig. 1B,D,F,G). As Nkx2.2 is assigned in the
135 more ventral region in the neural tube (Ribes and Briscoe, 2009), this finding suggests that the neural
136 progenitor cells acquired a more ventral identity by blockade of the PKA activity. While it has been
137 shown that the forced downregulation of the PKA activity ventralises the neural identities (Epstein et
138 al., 1996; Hammerschmidt et al., 1996; Vuolo et al., 2015), the explants treated with the sole H-89 did
139 not show any expression of Olig2 or Nkx2.2 (unpublished observation), suggesting that H-89 does not
140 have the function to mimic the Shh activity at least in this concentration.

141 Based on this observation, we investigated the relationship between the PKA activity and the
142 temporal change of the intracellular Shh signalling activity, and measured the Gli-activity at different
143 time points. We prepared pools of explants transfected with the *GBS-Luc* reporter construct (Sasaki et
144 al., 1999), which harboured the *luciferase* gene driven by the *Gli binding sequence* (*GBS*). We incubated
145 the explants with Shh^L or Shh^L with H-89 for 6 or 24 hours, and measured the Gli activities.

146 Consistent with the previous reports (Dessaud et al., 2010; Dessaud et al., 2007), we found the
147 upregulated Gli activity at 6 hours after the starting of the culture (Fig. 1H, lane 1). Importantly, the
148 activity level was comparable with the explants treated with Shh^L and H-89 (Fig. 1H, lane 2), suggesting
149 that the effect of H-89 was not evident at this time point. By contrast, at 24 hours, the Gli activity was
150 kept high in the explants with Shh^L and H-89, while the activation was almost undetectable in the
151 explants treated only with Shh^L (Fig. 1H, lanes 3 and 4). This observation suggests that the Gli activity
152 in the neural explants is sensitive to the PKA inhibitor only when cells are at the late (24 hours) time
153 point.

154 It has been suggested that the Gli3, a mediating transcription factor of Shh signal (Litingtung
155 and Chiang, 2000), is destabilised, and the total amount of the full-length and repressor forms of Gli3 is
156 therefore decreased by the treatment with Shh (Humke et al., 2010). Therefore, we determined whether
157 this amount was affected by the treatment with Shh^L or the culture period in the explants. We cultured
158 the explants either in the absence and in the presence of Shh^L for different time periods, and examined
159 them by western blots using the Gli3 antibody (Fig. 1I). When cells were treated with Shh^L for 6 hours,
160 both the full-length (Gli3FL) and repressor form of Gli3 (Gli3R) became less abundant, which is

161 consistent with the previous report that Gli3 is destabilised by Shh (Humke et al., 2010) (Fig. 1I, lanes
162 1 and 2, Fig. 1J). The same trend was found when H-89 was added with Shh^L (Fig. 1I, lanes 2,3, Fig.
163 1J). By contrast, in the explants cultured with Shh^L for 24 hours, the processing and the total amount of
164 Gli3 were more similar to those of the untreated explants (Fig. 1I, lanes 4,5, Fig. 1J), suggesting that the
165 temporal adaptation corresponds to the dynamic change of the Gli3 processing (Fig. 1H, lane 3).
166 However, this reversion of Gli3 processing by 24 hour-Shh^L was perturbed by H-89, suggesting that the
167 temporal Gli3 processing is sensitive to the PKA activity. The Gli3 processing did not significantly
168 change at 6 and 24 hours in the untreated explants (Fig. 1I, lanes 3 and 6, Fig. 1J), suggesting that the
169 PKA activity changes only when neural progenitor cells are exposed to Shh.

170 Taken together, the PKA activity changes over time and confers the temporal adaptation of the
171 Shh signal during the ventral neural differentiation.

172

173 **GPR17 is expressed in the ventral region of the neural tube**

174 Based on the observation in (Fig. 1), we supposed the existence of the PKA activity-
175 upregulating molecule(s) whose expression is dependent on Shh. To identify such molecules, we
176 focused on GPCRs, as many GPCRs regulate the activity of PKA and further modify the activities of
177 Gli transcription factors (Moore et al., 2016). With this in mind, we selected genes of GPCRs that can
178 bind to G α_s or G α_q , and performed a screen that combined RT-qPCR and *in situ* hybridisation (Fig. S2)
179 to isolate the GPCR that responds to Shh. Based on its expression pattern and responsiveness to Shh,
180 we identified the purinergic-like GPCR (a group of GPCRs that take purine as ligand) *GPR17* as a
181 candidate.

182 We first investigated the spatio-temporal expression of *GPR17* in the chick spinal cord, and
183 compared it with that of Olig2 and Nkx2.2 (Fig. 2A-F). *In situ* hybridisation analysis revealed that
184 *GPR17* was not expressed at HH stage10, immediately after the neural tube was formed and Olig2
185 started to be expressed (Fig. 2A,B). At HH stage 14, GPR17 was expressed broadly in the ventral region
186 covering the area where Olig2 and Nkx2.2 are strongly expressed (Fig. 2C,D). At HH stage 24, the
187 *GPR17* expression formed a dorsal-to-ventral gradient in the progenitor region of the neural tube, with
188 the lowest level at the dorsal region and highest level at Olig2- and Nkx2.2-positive regions, (Fig. 2E,F).
189 In addition, while the expression of *GPR17* was found in a wide area in the ventral region at the
190 beginning of the neural tube development (Fig. 2C), the floor plate expression halted as development
191 progressed (Fig. 2E,F).

192 In the mouse spinal cord, GPR17 expression was evident in the ventral region including pMN
193 and p3 areas at embryonic day 10.5 (e10.5) when neural tube pattern formation is taking place, as
194 confirmed both by *in situ* hybridisation and immunofluorescence (Fig. S3A-B). This expression pattern
195 was essentially the same as in the developing spinal cord of chicks.

196 To investigate the relationship between Shh and *GPR17* expression, we cultured the
197 intermediate neural explants in the presence of Shh^L or Shh^H (see Fig. S1 and Materials and Methods).
198 Expression levels of *GPR17* were measured by RT-qPCR, every 12 hours up to 48 hours (Fig. 2G). At

199 12 hours, *GPR17* expression was higher in explants treated with Shh^{L} or Shh^{H} than in untreated explants
200 (Fig. 2G), and this trend continued at 24 and 36 hours. By contrast, at 48 hours, expression was
201 downregulated in explants treated with Shh^{H} , but remained high in explants treated with Shh^{L} . This
202 finding is consistent with the *in vivo* expression pattern of abolished expression in the floor plate (Fig.
203 2E,F).

204 Next we explored the upstream transcription factors that induce *GPR17* expression. Since
205 *GPR17* requires *Olig1* for its expression (Abrajano et al., 2009; Chen et al., 2009) and is one of the
206 target genes of *Olig2* during oligodendrocyte development (Ou et al., 2016), we assessed if the
207 overexpression of an *Olig*-type transcription factors could induce the *GPR17* transcript. To address this,
208 we prepared intermediate neural explants that were electroporated with the *Olig2* expression plasmid,
209 and determined the *GPR17* expression level by RT-qPCR. *GPR17* expression was elevated at 24 hours,
210 suggesting that *Olig2* alone is sufficient to induce *GPR17* expression (Fig. 2H, lanes 1 and 2). By
211 contrast, *FoxA2*, characterising the floor plate, downregulated *GPR17* (Fig. 2E, lanes 1 and 3), which
212 was consistent with the observation that the *GPR17* expression was lower in the floor plate region.
213 *Znf488* (also known as *Zfp488*), which is expressed in the same regions as *Olig2* (Rehimi et al., 2016;
214 Wang et al., 2006), did not have a significant effect on *GPR17* expression (Fig. 2H, lanes 1 and 4).
215 These data supported the idea that *GPR17* expression is targeted by *Olig2* (Ou et al., 2016), and becomes
216 exclusive to the floor plate as development progresses.

217 We further investigated the requirement of *Olig2* for the expression of *GPR17*. We prepared the
218 neural explants electroporated with the construct encoding the dominant-negative version of *Olig2*
219 (Zhou and Anderson, 2002), and cultured with Shh^{L} for 24 hours (Fig. 2I). As a result, the *GPR17*
220 expression was downregulated, suggesting that the *GPR17* expression requires *Olig2* (Fig. 2I).

221 The collective results suggested that *GPR17* expression is mainly regulated by *Shh* signal and
222 its downstream transcription factor *Olig2*. This intriguing regulation of *GPR17* expression prompted us
223 to further investigate its role in neural tube development.

224

225 ***GPR17* is a negative regulator of the *Shh* signalling pathway**

226 We sought to characterise the molecular role of *GPR17* in the *Shh* signalling pathway, and first
227 analysed the subcellular localisation of *GPR17*. As *Shh* signal is mediated the membrane proteins
228 localised to the cilia (Sasai and Briscoe, 2012), we particularly focused on the correlation with the cilia.
229 However, in NIH3T3 cells, *GPR17* was not accumulated at the cilia in the normal culture condition (Fig.
230 S4A-C). This localisation did not change upon treatment with *Shh* (Fig. S4C). Moreover, in the mouse
231 neural tube, *GPR17* was not localised to the cilia of the apical surface. (Fig. S3C-G). Therefore the
232 subcellular localisation of *GPR17* does not have any correlation with the cilia.

233 Next we attempted to examine the effect of *GPR17* in the *Shh* intracellular signalling pathway.
234 For this purpose, we prepared control or *GPR17*-transfected NIH3T3 cells to assay the expression levels
235 of *Ptch1* and *Gli1*, which are primary target genes of the *Shh* signal (Cohen et al., 2015) (Fig. 3A). The
236 mere transfection of *GPR17* did not affect the expression levels of these genes (Fig. 3A). However,

237 when the cells were treated with Purmorphamine (Pur), an agonist of Smo, for 24 hours, the extent of
238 the upregulation in *GPR17*-transfected cells was significantly lower than in the control cells (Fig. 3A).
239 Given that Pur targets the Smo protein (Briscoe, 2006), this result suggests that GPR17 perturbs the
240 intracellular Shh signal at the downstream level of Smo.

241 We next sought to determine whether the amount of Gli3FL and Gli3R was affected by the
242 overexpression of *GPR17*. We treated the control or *GPR17*-transfected cells with Pur, and examined
243 them by western blots using the Gli3 antibody (Fig. 3B). Without Pur treatment, the ratio of the full-
244 length over the repressor form of Gli3 was not changed by the transfection of GPR17 (Fig. 3B, lanes 1
245 and 2). By contrast, when cells were treated with Pur, Gli3FL became less abundant (Humke et al.,
246 2010) (Fig. 3B, lane 3 and Fig. 3C). However, in the GPR17-expressing cells, the change in Gli3FL was
247 less than that of the control cells with Pur (Fig. 3B, lane 4 and Fig. 3C), suggesting that the effect of Pur
248 on Gli3 was perturbed by the presence of GPR17.

249 We further measured the cAMP levels in the cells, because modification of Gli3 proteins
250 depends on the intracellular cAMP level (Wang and Li, 2006). As a result, we found a higher cAMP
251 level in GPR17-overexpressed cells than in control cells (Fig. 3D). Furthermore, a reporter assay
252 measuring the activity of the cAMP-responsive element-binding region (CREB) displayed that the
253 transfection of the *GPR17* expression plasmid raised the CREB activity, confirming that the intracellular
254 cAMP level was raised upon the overexpression of *GPR17* (Fig. 3E). In cAMP-related assays (Fig.
255 3D,E), *GPR161* was used as a positive control (Mukhopadhyay et al., 2013).

256 Taken together, these findings demonstrated that GPR17 functions as a negative regulator of
257 the Shh signalling pathway by upregulating the cAMP level.

258

259 **GPR17 negatively regulates the ventral identity of the neural tube in a temporal manner**

260 To investigate the activity of GPR17 in neural tube development and pattern formation, we
261 overexpressed *GPR17* by *in ovo* electroporation in the neural tube of the chick embryos, and monitored
262 its effect on dorsal-ventral pattern formation. However, pattern formation was not significantly altered
263 (Fig. S5A-C"). This could be because a trigger (i.e. a ligand) is necessary to activate GPR17-mediated
264 signalling, and we speculated that the combination of GPR17 with its agonist, MDL29951 (Hennen et
265 al., 2013), would embody the phenotype of the *GPR17* overexpression.

266 To confirm that GPR17 and MDL29951 act synergistically, we administered a submaximal
267 level of MDL29951 onto the embryos, and found that the neural tube patterning was not changed (Fig.
268 S6A-C). By contrast, when MDL29951 was administered on the embryos overexpressed with GPR17,
269 the expression of Olig2 and Nkx2.2 was decreased in the electroporated cells, with the expansion of the
270 dorsal marker Pax7 (Fig. S6D-F"). This finding suggests that GPR17 acts synergistically with
271 MDL29951 in a cell-autonomous manner.

272 To find the effect of the GPR17-related signal in the dorsal-ventral patterning of the whole
273 neural tube, we employed New culture system, in which embryos were cultured *ex ovo* (Psychoyos and
274 Finnell, 2008). The embryos were cultured in the absence or in the presence of an effective level of

275 MDL29951. As a result, the ventral neural domains characterised by *Olig2* and *Nkx2.2* were
276 significantly reduced (Fig. 4A-D), while the *Pax7*-expressing area was expanded (Fig. 4E,F), with the
277 decreasing expression of *Ptchl* (Fig. 4G,H), suggesting that the ventral neural differentiation was
278 abrogated. By contrast, *FoxA2* and *Shh* expression was intact (Fig. 4I-L), suggesting that perturbation
279 of the dorsal-ventral pattern was arisen by the change of characters of neural progenitor cells, rather
280 than the alteration of the expression level of *Shh*.

281 Next, to reveal the relationship between the intracellular *Shh* signal and *GPR17* more directly,
282 we conducted an explant analysis. Because the expression of *GPR17* is induced by *Shh* and *GPR17*
283 negatively regulates the *Shh* signal activity at the intracellular level (Fig. 2G,3A), we reasoned that
284 *GPR17* is involved in temporal regulation of *Gli* activity (Balaskas et al., 2012; Dessaud et al., 2010;
285 Dessaud et al., 2007). To test this hypothesis, we measured the *Gli* activity over time. At 6 hours, the
286 *Gli* activity was comparable in the explants treated with Shh^{H} in the absence and presence of 30 μM of
287 MDL29951 (Fig. 4M lanes 1,2). However, at the 24-hour time point, the explants added with
288 MDL29951 along with Shh^{H} displayed a significantly reduced level of *Gli* activity than in those without
289 MDL29951 (Fig. 4M). These data suggest that the temporal *Gli* activity was perturbed by *GPR17* and
290 its related signals.

291 As the *Gli* activity was decreased in the Shh^{H} explants by MDL29951, we expected that the
292 neural identities was altered as well. Shh^{H} treatment of the explants for 24 hours simulated the
293 differentiation into ventral neural progenitor cells; *Nkx2.2* expression was detectable in the majority of
294 cells, and *Olig2* in a smaller subset (Fig. 4N,P,R,T). By contrast, when the explants were treated with
295 MDL29951 along with Shh^{H} , the number of cells expressing *Nkx2.2* decreased, whereas *Olig2*-positive
296 cells increased (Fig. 4O,Q,S,T). Given that the *Olig2*-expressing cells can be induced by a lower
297 concentration of *Shh* (Dessaud et al., 2007), the results are consistent with the one from the measurement
298 of the *Gli* activity, and *Shh* was partially inhibited by the *GPR17*-associated signalling. This tendency
299 was confirmed by using the *Smo* agonist *Pur*. 500 nM of *Pur* induced a large number of *Nkx2.2*-positive
300 cells, while the treatment together with MDL29951 reduced the *Nkx2.2*-positive cells and increased the
301 *Olig2*-expressing cells (Fig. S6G-M). This result supports the idea that *GPR17*-related signal negatively
302 regulates the effect of *Shh*.

303 Next, the same analyses were performed with the Shh^{L} -treated explants. As in the case of Shh^{H} ,
304 the *Gli* activity was comparable at 6 hours (Fig. S6N). In addition, at 24 hours, the activity in the
305 MDL29951-treated Shh^{L} explants was at a similar level to those without MDL29951. Consistently, the
306 assignment of the neural identities was not altered; *Olig2*-expressing cell dominated regardless of the
307 MDL29951 treatment (Fig. S6O-U). Given that the *Gli* activity is downregulated quickly in the
308 condition of Shh^{L} (Dessaud et al., 2010; Dessaud et al., 2007), this result suggests that MDL29951 did
309 not exert a significant blocking effect on the Shh^{L} , and the collective results above suggest that *GPR17*-
310 related signal perturbed the *Gli* activity in a time-dependent manner.

311 It is unlikely that the alteration of the pattern formation is mediated by the programmed cell
312 death, as a TdT-mediated dUTP nickend labelling (TUNEL) assay did not detect a significantly
313 increased number of positive signals either in the explants (Fig. S7A-C).

314 We attempted to further investigate if the activation of the GPR17-related signal correlated with
315 the elevation of the intracellular cAMP level in the intermediate neural explants. Consistent with the
316 previous observation (Hammerschmidt et al., 1996; Humke et al., 2010; Moore et al., 2016), the cAMP
317 level in the explants treated with Shh for 24 hours showed a lower cAMP level than in the control
318 explants (Fig. 4U, lanes 1,2). However, in the explants treated with MDL29951 in combination with
319 Shh, this level was restored (Fig. 4U, lanes 1,3), suggesting that MDL29951 perturbed the Shh-mediated
320 decrease in the cAMP level.

321 The regulation of the cAMP level by the GPR17-related signal occurred at the upstream level
322 of PKA, because the ventralising effect induced by the dominant-negative PKA (dnPKA) could not be
323 reverted by the coelectroporation with GPR17 followed by the administration of MDL29951, as
324 confirmed by the expression of Nkx2.2 (Fig. S7D-E”).

325 Together, these findings suggested that the GPR17-mediated signalling pathway negatively
326 regulates Shh activity in the context of neural tube pattern formation through the upregulation of the
327 intracellular cAMP level.

328

329 **Perturbation of GPR17 expression causes aberrant expansion of ventral progenitor domains**

330 To further investigate the functions of GPR17 in the development of neural tube pattern
331 formation, we employed a loss-of-function approach. For this purpose, we designed two *siRNAs*
332 targeting GPR17 (*si-GPR17-1* and *si-GPR17-2*), and carried out *in ovo* electroporation into the neural
333 tube.

334 We first electroporated *si-GPR17* into the neural tube at HH stage 12. At 48 hpt, we observed
335 aberrant expansion of the ventral neural domains characterised by Olig2, Nkx2.2, FoxA2 and the motor
336 neuron domain identified by Islet1 (Fig. 5A-H”). Moreover, probably because the low level expression
337 of *GPR17* was perturbed by *si-GPR17*, the area positive for Pax7 expressed in the dorsal progenitor
338 domains was diminished (Fig. 5I-J”). This finding suggested that GPR17 *per se* is a negative regulator
339 of the Shh signal. This aberrant expression was abolished by co-electroporation of mouse *GPR17*, which
340 is not targeted by *si-GPR17* (Fig. S5D-F”), suggesting that the phenotype observed in *si-GPR17*
341 transfection was due to downregulation of *GPR17* expression. Furthermore, co-electroporation of
342 *GPR161*, another negative regulator of the Shh signalling pathway (Mukhopadhyay et al., 2013), did
343 not abolish the phenotypes caused by *si-GPR17*, confirming the specificity of *si-GPR17* (Fig. S5G-I”).
344 The expansion of ventral identity was also observed when *si-GPR17-2* was electroporated into neural
345 tubes (Fig. S8), validating the phenotype. Thus, GPR17 was demonstrated to be a negative regulator of
346 the intracellular Shh signalling, and is essential for proper pattern formation in the neural tube.

347

348 **GPR17 is essential for dynamic control of Shh activity**

349 Finally, we investigated if GPR17 plays an essential role for the temporal regulation of Gli
350 activity (Balaskas et al., 2012; Dessaud et al., 2010; Dessaud et al., 2007).

351 First, we asked if the intracellular Shh signal activity was aberrantly upregulated, and prepared
352 intermediate neural explants electroporated with *si-GPR17*, and then treated them with Shh^L. Although
353 Olig2-expressing cells were predominant in the *si-control* electroporated explants (Fig. 6A-D,I), a
354 significantly higher population of Nkx2.2-positive cells appeared at 24 hours in the *si-GPR17*
355 electroporated explants (Fig. 6E-H,I), suggesting that the intracellular Shh signal activity was
356 upregulated when *GPR17* expression was reduced. This observation was supported by the effect of
357 treatment with pranlukast, a chemical antagonist of GPR17 (Hennen et al., 2013; Parravicini et al.,
358 2010); explants treated with 10 μM pranlukast in combination with Shh^L tended to contain larger
359 proportions of Nkx2.2-positive cells than controls, suggesting that perturbation of GPR17 caused the
360 more ventral identity (Fig. S9A-G).

361 We next sought to analyse dynamic control of the intracellular Shh signal activity during ventral
362 neural differentiation. For this purpose, we performed luciferase reporter assays using *GBS-Luc* at
363 various time points. We prepared explants electroporated with *GBS-Luc* with either *si-control* or *si-*
364 *GPR17*, and then measured Gli activity at a series of time points from 6 to 48 hours after the initiation
365 of the culture. In *si-control*-electroporated explants treated with Shh^L, Shh activity gradually decreased
366 over time, peaking at 6 hours and becoming undetectable by the 48 hour time point (Fig. 6J, blue line),
367 consistent with previous reports (Dessaud et al., 2010; Dessaud et al., 2007). On the other hand, in
368 explants with *si-GPR17*, Gli activity at 6 hours was comparable to that of the *si-control* explants, but
369 the activity was significantly higher at 24 hours and still detectable at 36 hours (Fig. 6J, red line).

370 We next attempted to confirm that the dynamic Gli activity reflects the gene expression. We
371 therefore cultured the explants electroporated with *si-control* or *si-GPR17* in the presence of Shh^L for
372 different time periods, and measured the expression levels of *Ptch1* and *Gli1* by RT-qPCR. As the result,
373 the expression peaked at 12 hours and then decreased quickly at 24 hours in *si-control* electroporated
374 explants (Fig. 6K, Fig. S9H, blue lines). However, in the *si-GPR17*-electroporated explants, while the
375 expression at 12 hours was comparable, the decrease was delayed, and the expression level was
376 significantly higher at 24 hours (Fig. 6K, Fig. S9H, red lines). The successful perturbation of *GPR17*
377 expression was confirmed by RT-qPCR against the GPR17 primers (Fig. S9I). This result supports the
378 idea that the dynamic Gli activity was affected by the perturbation of the GPR17 expression.

379 We further asked if the dynamic Gli activity corresponds to the processing the Gli3 protein. For
380 this purpose, we performed western blots with the Gli3 antibody in the chick explants electroporated
381 with either *si-control* or *si-GPR17*. At 6 hours, the Gli3 protein processing was significantly affected by
382 the treatment with Shh both in *si-control*- and *si-GPR17*-transfected cells (Fig. 6L, left panel, and Fig.
383 6M). By contrast, at 24 hours, while the *si-GPR17*-electroporated explants did not change the Gli3
384 processing in the absence of Shh (Fig. 6L, lanes 5 and 6, Fig. 6M), the *si-GPR17*-explants had the
385 significantly destabilised Gli3 than in the *si-control*-explants upon the treatment with Shh (Fig. 6L, lanes
386 7 and 8, Fig. 6M), suggesting that GPR17 affects on the temporal processing of Gli3.

387 Together, these findings indicate that GPR17 is an essential upstream factor that controls the
388 dynamic change between the full-length and repressor forms of Gli3, and thus regulates the temporal
389 change in the intracellular Shh signalling activity.

390

391 **GPR17 affects cell fate determination in neural differentiation from mouse ES cells**

392 We finally assessed whether GPR17 functions are conserved in different organisms by
393 investigating its functions in aspects of mouse development.

394 For this analysis, we examined the directed neural differentiation of the ES cells, because the
395 effects of treatments on gene expression are easily evaluated in this system. Mouse ES cells were
396 differentiated into neural subtypes of pMN, p3 and floor plate using different combinations of retinoic
397 acid (RA) and SAG, as described previously (Fig. S10A) (Kutejova et al., 2016). First, we evaluated
398 GPR17 expression by RT-qPCR in each neural subtype. The results revealed significantly higher GPR17
399 expression in pMN and p3 cells than in FP 5 days after the start of differentiation (day 5) (Fig. 7A),
400 suggesting that expression can be recapitulated in neural cells differentiated from ES cells.

401 By using this differentiation protocol, we analysed the effect of GPR17-related signal in the
402 neural fate determination. During the differentiation into pMN, MDL29951 was added at day 3.5 and
403 gene expression was evaluated at day 5.

404 In the pMN condition, the majority of cells expressed Olig2, with a small subset of Pax6-
405 positive cells, as demonstrated by immunofluorescence (Fig. 7B,D,F). By contrast, the cells treated with
406 MDL29951 displayed significantly larger number of Pax6-positive cells with reduced number of Olig2-
407 positive cells (Fig. 7C,E,F), suggesting that the Shh signal was partially perturbed and cells obtained
408 more dorsal identity.

409 Conversely, we sought to analyse the essential function of GPR17 in neural differentiation and
410 subtype determination, and transfected two different *si-RNAs* (*si-GPR17-1* and *si-GPR17-2*) targeting
411 *GPR17* in ES cells. The efficient knockdown of *GPR17* expression was validated by RT-qPCR (3
412 experiments; Fig. S10B).

413 Under these conditions, ES cells were differentiated into pMN cells, and gene expression was
414 evaluated on day 5. In the pMN condition, the majority of cells expressed Olig2, with a small subset of
415 Nkx2.2-positive cells, as demonstrated by immunofluorescence (Fig. 7G,J,M,P). By contrast, treatment
416 with *si-GPR17* increased the Nkx2.2-expressing cells (Fig. 7H,I,K,L,N,O,P). This observation suggests
417 that *si-GPR17*-treated cells became more susceptible to the Shh ligand and tended to differentiate into
418 the more ventral identity of p3 (Fig. S10C-E), for which a higher Gli activity was required (Kutejova et
419 al., 2016).

420 We next verified this tendency by RT-qPCR. In cells treated with *si-GPR17s*, the *Nkx2.2*
421 expression was higher than in *si-control*-transfected cells at day 5, confirming the results obtained by
422 the immunofluorescence (Fig. 7Q). Furthermore, the expression level of *Ptch1*, a target gene of the Shh
423 signal, was higher in *si-GPR17* cells than in the controls (Fig. 7Q). These results were consistent with
424 the findings obtained in the analyses of chick embryos.

425 These findings suggest that mouse GPR17 is expressed in the pMN and p3 cells differentiated
426 from ES cells as in the chick embryos, and functions as a modulator for the ventral identities of the
427 neural cells.

428 **Discussion**

429 **GPR17 is a negative regulator of the Shh signalling pathway and affects ventral pattern formation**
430 **of the neural tube**

431 In this study, we demonstrated that the temporal change of the PKA activity in the neural
432 progenitor cells confers the temporal adaptation against Shh (Fig. 1), and isolated GPR17 as a modulator
433 for this temporal activity (Fig. 3D,3E,4U). Although its expression is induced by Shh, GPR17 negatively
434 regulates the Shh signal, thereby affecting the dynamicity of the Gli activity (Dessaud et al., 2010;
435 Dessaud et al., 2007). Negative regulation of the intracellular Shh signal by GPR17 is conserved in the
436 mouse, as demonstrated by a system involving neural differentiation of ES cells (Fig. 7).

437 GPR17 was initially recognised as one of the genes that respond to neural tube injury, brain
438 damage or pathological situations (Ceruti et al., 2009; Ciana et al., 2006; Lecca et al., 2008). A previous
439 study using the mutant mice revealed that the deficiency of the *GPR17* gene caused the earlier
440 differentiation and excessive production of oligodendrocyte cells, suggesting that GPR17 determined
441 the timing of oligodendrocyte differentiation (Chen et al., 2009). Subsequent studies have established
442 the idea that GPR17 regulates the proliferation and differentiation of oligodendrocyte precursor cells
443 (Lu et al., 2018; Merten et al., 2018). Given that oligodendrocyte differentiation is supported by Shh
444 (Oh et al., 2005), the phenotypes caused by the alteration of the GPR17 expression may be mediated by
445 the modulation of the Gli activity (Chen et al., 2009).

446 Although GPR17 has been suggested to be a receptor for the uracil nucleotides and Cysteinyl
447 leukotrienes (cysLTs) (Ciana et al., 2006; Fumagalli et al., 2016; Lecca et al., 2008), the actual ligand(s)
448 for GPR17 working in the developmental contexts have not been identified. In this study, we utilised
449 MDL29951 to experimentally activate GPR17 (Fig. 4L,N,P,E-U, Fig. S6A-F", S7E-S7E", S7J-S7J").
450 While MDL29951 has been recognised as an agonist of GPR17 (Hennen et al., 2013) and was actually
451 used to analyse the function of GPR17 (Ou et al., 2016), MDL29951 has also been recognised as an
452 antagonist of the N-methyl-D-aspartate (NMDA) receptor (Heppenstall and Fleetwood-Walker, 1997;
453 Jansen and Dannhardt, 2003). However, as we demonstrated, MDL29951 synergistically acted with
454 GPR17 at least in the context of the dorsal-ventral patterning (Fig. S4).

455 The *in vivo* functions of GPR17 in the mouse CNS development is an open question; at least,
456 GPR17 is not critical for the embryonic development (Chen et al., 2009; Lu et al., 2018; Merten et al.,
457 2018), as *GPR17*-deficient mice are viable. This is probably due to the redundant roles of the multiple
458 factors expressed in the mouse neural tube. One of such candidates is *Adenylyl cyclase 5 (AC5)*, which
459 catalyses the dissociation of ATP to make cAMP (Moore et al., 2016; Vuolo et al., 2015). As we found
460 that *AC5* expression was induced by Shh both in chick and mouse neural explants (Fig. S11), the
461 regulatory mechanism of *AC5* (and its related factor *AC6*) is similar to that of GPR17. It is possible that
462 GPR17 and other factors work in concert with each other to regulate the temporal adaptation of Shh,
463 and the dependency on each gene is species-specific.

464 GPCRs can bind to different types of $G\alpha$ proteins, including $G\alpha_i$, $G\alpha_s$, $G\alpha_q$ and $G\alpha_{12,13}$
465 (Rosenbaum et al., 2009). Among these $G\alpha$ proteins, $G\alpha_q$ and $G\alpha_s$ can increase the intracellular cAMP

466 level, whereas $G\alpha_i$ proteins mostly exert an inhibitory effect, and GPR17 can bind all types of G-proteins
467 (Hennen et al., 2013). During the remyelination, GPR17 binds to $G\alpha_i$ and decreases the cAMP level
468 (Buccioni et al., 2011; Ou et al., 2016; Parravicini et al., 2008; Simon et al., 2016). By contrast, in our
469 experiments GPR17 rather upregulated the cAMP level (Fig. 2G), presumably by binding to $G\alpha_q$ and/or
470 $G\alpha_s$, suggesting that it has diverse and cell type-specific functions.

471

472 **GPR17 constitutes a negative feedback loop of the Shh signalling system**

473 A historical model suggested that a morphogen can produce a number of cell types depending
474 on the thresholds of the signal concentration (Wolpert, 1969). This hypothesis relies on the supposition
475 that signal concentration completely corresponds to the intracellular signal intensity. However, recent
476 studies suggest that the temporal change in signal activity, so-called temporal adaptation, is critical for
477 cell fate determination and correct pattern formation (Dessaud et al., 2010; Dessaud et al., 2007; Ribes
478 and Briscoe, 2009). The results of this study reveal a novel negative feedback loop constructed by a
479 GPCR through regulation of the intracellular cAMP level and processing of Gli transcription factors
480 (Fig. 1). Recent mathematical modelling suggests the existence of negative regulators induced by Shh
481 (Cohen et al., 2015), and our findings regarding GPR17 are in good agreement with this hypothesis.

482 The function of GPR17 is to modulate the intracellular cAMP level (Fig. 3D, 4U). In this study,
483 we analysed the processing of Gli3 to evaluate the Gli activity (Fig. 1I, 3B, 6L), Gli2 has been shown
484 to play essential roles for the dorsal-ventral pattern of the neural tube. (Pan et al., 2009) Therefore, the
485 analysis on the dynamics of Gli2 processing may also be intriguing in a future study.

486 Although Shh induces the *GPR17* expression (Fig. 2G), *GPR17* does not seem to be a direct
487 target gene of Gli transcription factors, as *GBS* has not been identified in the flanking regions of the
488 *GPR17* gene locus (Kutejova et al., 2016). Instead, Olig2 is the direct regulator of *GPR17* expression
489 (Ou et al., 2016). Consistent with this finding, overexpression of Olig2 in neural explants induces
490 *GPR17* expression (Fig. 2H). This could explain why the negative feedback regulation is cell type-
491 specific and does not take place in the NIH3T3 cells treated with the Shh ligand (Cohen et al., 2015);
492 Olig2 expression is induced only in the neural progenitor cells, but not in NIH3T3 cells (AY, AH, NS;
493 unpublished observation).

494 In a developmental context, negative feedback regulation confers diversity of cell types and
495 robustness of pattern formation (Dessaud et al., 2010). To date, multiple negative feedback systems for
496 the Gli activity have been identified (Cohen et al., 2015). For instance, the *Ptch1* gene, whose product
497 negatively regulates the intracellular Shh signal activity, is a direct target of Shh (Fig. 8) (Dessaud et al.,
498 2007). Moreover, expression of the transcriptional mediator Gli2 decreases over time during neural
499 development, although the underlying regulatory mechanisms remain elusive (Cohen et al., 2015). In
500 combination with the existence of GPR17 as this study demonstrated (Fig. 8), multiple negative
501 feedback systems could cause differences in the half-life of the signal in each progenitor cell, allowing
502 diverse cell types to be produced by a single morphogen, Shh. Moreover, during formation of the
503 morphogen gradient, uncertainties and fluctuations may arise. This noise in the signal is constantly

504 modulated by negative feedback, and consequently the reliability and reproducibility of pattern
505 formation can be incarnated (Lander, 2011; Perrimon et al., 2012). Therefore, the negative feedback
506 loop formed by Shh and GPR17 is important not only for overall neural tube pattern formation, but also
507 for fine tuning of signal intensity, and consequently establishes the quantitative balance among different
508 cell types during neural and neuronal differentiation. Further studies, including analysis of the temporal
509 change of intracellular cAMP level, will reveal the significance of GPR17 in negative feedback of the
510 Shh signal.

511 **Materials and Methods**

512 **Isolation of GPR17**

513 GPCRs that can couple with $G\alpha_q$ or $G\alpha_s$ were identified by referring to the website
514 (<http://gpcrdb.org>), and qPCR primers were designed against the corresponding genes (Tab. S1).
515 Relative expression levels were analysed by RT-qPCR in neural explants treated or untreated with Shh^H
516 (Fig. S1). NCBI Gene IDs for chicken and mouse *GPR17* are 769024 and 574402, respectively.

517

518 **Embryos, electroporation and expression analysis**

519 All animal experiments were performed with the approval of the Animal Welfare and Ethical
520 Review Panel of Nara Institute of Science and Technology (approval numbers 1636 and 1810 for
521 chicken and mouse experiments, respectively). Chicken eggs were purchased from the Shiroyama Kei-
522 en farm (Kanagawa prefecture, Japan) and the Yamagishi farm (Wakayama prefecture, Japan), and the
523 developmental stages were evaluated by the Hamburger and Hamilton's criteria (Hamburger and
524 Hamilton, 1992). *In ovo* electroporation of chick embryos was carried out with an ECM830
525 electroporator (BTX), and embryos were incubated at 38°C for the indicated times. Overexpression in
526 the chick embryos was performed with the constructs subcloned into the *pCIG* expression plasmid,
527 which contains an IRES (internal ribosomal entry site) -GFP gene downstream of the gene of interest
528 (Megason and McMahon, 2002). *pCIG-Olig2^{DBD}-VP16* was constructed by fusing the DNA-binding
529 region of Olig2 with the transactivation domain of the viral protein VP16, as described previously (Zhou
530 and Anderson, 2002; Zhou et al., 2001). Embryos were fixed with 4% paraformaldehyde, subsequently
531 incubated with 15% sucrose for cryoprotection and embedded in 7.5% gelatine (Sigma). Cryosections
532 were cut at 14 µm increments and analysed with immunofluorescence or *in situ* hybridisation. The
533 sections from at least five independent embryos were analysed, and the number of the embryos analysed
534 were indicated in the text. For loss-of-function experiments, *si-cGPR17-1*
535 (GGAACAGAGUGGAGAAACACCUG(dA)(dA) (sense) and
536 UUCAGGUGUUUCUCCACUCUGUCCCA (antisense)) or its negative control *si-control*
537 (AUGCUUCUCCGAACGUGUCACGU(dT)(dT) (sense) and
538 UUUCGUGACACGUUCGGAGAAGCAUCA (antisense); Eurofin) and *si-cGPR17-2*
539 (CAGACUGUGGAAGUGAACACACAA) or *si-control* (siRNA Negative Control, Med GC;
540 Invitrogen) was electroporated with the *pCIG* vector, which encodes *GFP* as a tracer. Unless mentioned
541 otherwise, loss-of-function experiments were performed with *si-cGPR17-1*.

542 DIG-labelled (Roche) complementary RNA probe was synthesised using RNA polymerase
543 (Promega). *In situ* hybridisation on slides was performed as described previously (Sasai et al., 2014).

544 Immunofluorescence was performed as described previously (Sasai et al., 2014). Primary
545 antibodies against the following proteins were used in this study: Olig2 (rabbit, Millipore AB9610),
546 Nkx2.2 (mouse, DSHB 74.5A5; rabbit, Abcam ab19077), Islet1/2 (DSHB 39.4D5), Pax7 (DSHB),
547 FoxA2 (goat, Santa Cruz sc-6554X), Sox2 (rabbit, Millipore AB5603), GPR17 (goat, Abcam ab106781
548 for mouse embryos; rabbit, Sigma SAB4501250 for cells), GFP (sheep, AbD Serotec 4745-1051), Gli3

549 (goat, R&D AF3690), β -Actin (rabbit, Abcam ab8227), and γ -acetylated tubulin (mouse, Sigma T7451).
550 For GPR17 immunofluorescence in mouse embryonic sections, antigenic retrieval was required; slides
551 were boiled for 1 minute in 10 mM of citric acid (pH 6.0) solution prior to the incubation with the
552 primary antibody. Fluorophore- and HRP-conjugated secondary antibodies were purchased from
553 Jackson Laboratory and Cell Signaling Technology, respectively.

554

555 **New culture and intermediate neural explants**

556 New culture was performed as described previously (Psychoyos and Finnell, 2008). Culture
557 plates containing albumen and agarose were prepared with the final concentration of 100 μ M of
558 MDL29951 or with dimethylsulfoxide (DMSO) (control). Chick embryos were taken from the eggs at
559 HH stage 12 with a ring of filter paper, and put on the culture plates with the ventral side up. Embryos
560 were cultured in the 38°C incubator for 36 hours, and the plates were kept humid with Hanks' Balanced
561 Salt solution (1xHBSS; Sigma-Aldrich).

562 Chick intermediate neural explants were prepared as described previously (Sasai et al., 2014).
563 HH stage 9 embryos were isolated from the eggs and maintained in L-15 medium (Thermo Fisher
564 Scientific). After treatment with Dispase II (Sigma), the intermediate region of the neural plate at the
565 preneural tube level (Delfino-Machin et al., 2005) was manually excised from the embryos and cultured
566 in DMEM/F-12 medium (Thermo Fisher Scientific) supplemented with Mito+Serum Extender (Sigma)
567 and penicillin/streptomycin/glutamine (Wako). The explants were cultured in the pH-adjusted collagen
568 gel (Sigma; for immunofluorescence and RT-qPCR) or on the glass plates coated with gelatin (Sigma;
569 for western blots). Quantitation of positive cells was performed at least five areas, each of which
570 contained approximately 200-250 cells, randomly chosen from independent explants. Shh^L and Shh^H
571 were defined as the concentrations of Shh that differentiate explants into motor neuron and floor plate
572 at 48 hours, respectively (Fig. S1). Shh^H is 4 times as high as Shh^L . H-89 (Wako) and MDL29951 were
573 used at the indicated concentrations. For RT-qPCR analyses, RNA was extracted from the pools of 15
574 chick intermediate neural explants by using PicoPure RNA extraction kit (Thermo Fisher Scientific).
575 Each extraction gave a range of 500 ng (12-hour culture) to 1.5 μ g (48-hour culture) of total RNA, as
576 measured by Nanodrop (Thermo Fisher Scientific). Complementary DNAs (cDNAs) were synthesised
577 by PrimeScript reverse transcriptase (TaKaRa), and qPCR was performed by using LightCycler 96
578 (Roche). At least two independent pools of explants were analysed in each experiment, and each gene
579 expression level was normalised with the *GAPDH* expression.

580 Mouse neural explants (Fig. S11) were prepared from the e8.5 embryos and were cultured in
581 the same way as in the chick explants (Balaskas et al., 2012), except that the culture medium contained
582 N2 and B27 supplements (Thermo Fischer Scientific).

583

584 **Cell culture, transfection and selection**

585 NIH3T3 fibroblast cells were maintained in Dulbecco's modified Eagle's medium /F12 medium
586 (Wako) containing 10% New-Born Calf Serum (MP Biomedicals). Lipofectamine 3000 (Invitrogen)

587 was used for transfection. To obtain explicit evidence of the effects on the overexpression of the genes
588 in Fig. 3E-I, the transfected cells were selected for 48 hours with 500 µg/ml of G418 (Invitrogen) from
589 one day after the *pcDNA3*-based expression plasmids were transfected, and were used for assays.

590

591 **Monitoring the Gli activity and the intracellular cAMP levels**

592 The *GBS-Nano-Luc* reporter construct containing the *GBS* was constructed by subcloning of the
593 octameric *GBS* (Sasaki et al., 1999) to the pNL3.2 vector (Promega), and used to monitor Gli activity.
594 *pCS2-firefly luciferase* was used for an internal control. For the luciferase assays on chick neural
595 explants, *GBS-Nano-Luc* and *pCS2-firefly-luciferase* were electroporated at the preneural tube region of
596 the caudal part of the chick embryos at HH stage 9- (Delfino-Machin et al., 2005). *si-RNAs* were co-
597 electroporated if necessary. The explants were then prepared and were cultured with the indicated
598 conditions. The relative luciferase activities were compared to those cultured without Shh at every time
599 point. 7-8 explants were grouped for each measurement, and four to 10 groups of explants were
600 measured in one condition.

601 *CREB-Luc* (luciferase gene driven by the cAMP-responsive element-binding region) was a kind
602 gift from Prof. Itoh (Jenie et al., 2013) and *pRL-CMV* (Promega) was used for an internal control. The
603 measurement of the chemiluminescence was performed by using the plate reader Tristar2 (Berthold
604 Technologies).

605 For the cAMP assay in the NIH3T3 cells (Fig. 3D), the cells were transfected with the indicated
606 plasmids and the transfected cells were selected for 24 hours. 3-isobutyl-1-methylxanthine (IBMX), a
607 non-competitive selective phosphodiesterase inhibitor, was added at 1 µM in the last 30 minutes before
608 cells were harvested to raise the basal level of intracellular. For the cAMP assay in the neural explants
609 (Fig 4U), 15 explants were prepared for each condition and cultured for 24 hours. IBMX was added in
610 the last 1 hour. The cAMP assay was performed using DetectX high sensitivity direct cAMP
611 Chemiluminescent Immunoassay Kit (Arbor Assays). The protein concentrations of the cell lysates were
612 measured by CBB protein assay solution (Nacalai, Japan) and the measurement values were normalised.

613

614 **TUNEL assay**

615 TUNEL assay was performed to detect the apoptotic cells. The neural tube sections or the explants were
616 incubated with TdT transferase (Roche) and DIG-labelled dUTP (Merck Millipore), and the signals
617 were visualised by anti-Digoxigenin-Rhodamine antibody (Sigma). Staurosporine (Belmokhtar et al.,
618 2001) was used as a positive control at 1 nM.

619

620 **Neural differentiation of mouse ES cells**

621 The Sox1-GFP ES cell line was kindly provided by Prof. Smith, and maintenance and neural
622 differentiation as a monolayer culture were performed as described previously (Kamiya et al., 2011;
623 Kutejova et al., 2016; Ying et al., 2003). Briefly, on the fibronectin/collagen-coated plates,
624 approximately 1.5×10^4 ES cells were seeded and cultured as monolayers in the differentiation medium

625 (Kutejova et al., 2016) for the initial 3 days. For pMN differentiation, cells were added with 300 nM RA
626 (Sigma) on day 3.0 and 50 nM SAG was added on day 3.5; and the cells were incubated for totally 5
627 days. For p3 differentiation, 30 nM RA and 500 nM SAG (Sigma) were added on day 3.0 and day 3.5,
628 respectively. For FP differentiation, 500 nM SAG was added on day 3.0. Before differentiation was
629 initiated, Stealth *siRNAs* (Invitrogen) (*si-mGPR17-1*, UGCCUGCUUCUACCUUCUGGACUU; *si-*
630 *mGPR17-2*, ACCGUUCAGUCAUGUGCUUCACUA) or *si-control* (Invitrogen) were transfected
631 twice at 24 hour intervals using Lipofectamine RNAiMAX (Invitrogen). For RT-qPCR analysis, RNA
632 was extracted by RNeasy RNA extraction kit (QIAGEN). cDNA synthesis and qPCR were performed
633 as in the chick neural explants.

634

635 **Images and data analysis**

636 Images were collected by using AxioVision2 (for *in situ* hybridisation images; Zeiss), LSM 710
637 confocal microscope (for immunofluorescence data; Zeiss), LAS4000 (for western blots; GE
638 Healthcare), and signal intensities of the western blots were calculated by ImageJ. Images were
639 processed by the software Photoshop (Adobe) and figures were arranged on Illustrator (Adobe).
640 Statistical analysis was performed with Prism (GraphPad) with two-tailed t-test (Fig. 1J,
641 2H,3A,3C,3D,4M,4T,6I,6J,6K,7F,7P,7Q) or with one-way analysis of variance (ANOVA) followed by
642 Tukey's post-hoc test (Fig. 1H,1J,2I,3E,4U,6M,7A), and data are presented as mean values \pm s.e.m.,
643 and significance (*; $p < 0.05$; **, $p < 0.01$, ***, $p < 0.001$, ****, $p < 0.0001$ or n.s.; not significant) were
644 indicated in each graph.

645

646 **Acknowledgements**

647 The authors are grateful to Profs. Austin Smith and Hiroshi Itoh for materials, Dr. James Briscoe
648 for comments on the manuscript, Prof. Naoyuki Inagaki, Drs. Yuichi Sakumura and Takunori Minegishi
649 for advice, Prof. Takashi Toda for encouragement, and all laboratory members for support and valuable
650 discussion.

651

652 **Funding**

653 This study was supported in part by grants-in-aid from Japan Society for Promotion of Science
654 (15H06411, 17H03684; NS) and from MEXT (19H04781; NS); the Joint Research Program of the
655 Institute for Genetic Medicine, Hokkaido University (TK, NS); the Takeda Science Foundation (NS,
656 AH); the Mochida Memorial Foundation for Medical and Pharmaceutical Research (NS); the Ichiro
657 Kanehara Foundation for the Promotion of Medical Sciences and Medical Care (NS); the Uehara
658 Memorial Foundation (NS); and the NOVARTIS Foundation (Japan) for the Promotion of Science (NS).

659

660 **Competing interests**

661 The authors have declared that no competing interests exist.

662

663 **Author contributions**

664 NS conceived the project. AY, AH, MK, NS performed experiments and analysed the data.

665 MMT, TK provided essential materials and advice. All authors joined the discussion and NS wrote the

666 manuscript.

667 **Figure Legends**

668 **Fig. 1. Temporal change of the intracellular cAMP level confers the temporal adaptation of the**
669 **neural progenitor cells.**

670 (A-G) The intermediate neural explants cultured with Shh^L (A,C,E,G) or with Shh^L + H-89 (2 μ M;
671 B,D,F,G) for 24 hours were analysed by immunofluorescence with Olig2 (A,B,E,F) and Nkx2.2
672 (C,D,E,F) antibodies. (G) Quantitative data for (A-F). (H) Temporal Gli activities are altered by
673 blocking the PKA activity. Explants electroporated with *GBS-Luc* were incubated with Shh^L or Shh^L +
674 H-89 for 6 or 24 hours, and luciferase activities were measured. (I) The processing of the Gli3 protein
675 corresponds to the Gli activities. Western blot analysis was performed in the explants cultured with Shh^L
676 or Shh^L + H-89 for 6 or 24 hours, as in (H). The full-length (FL) and repressor (R) forms of Gli3 were
677 indicated with arrowheads. (J) The total amounts of Gli3FL and Gli3R in (I) were quantified. Scale Bars
678 in (A) for (A-F) = 50 μ m

679

680 **Fig. 2. GPR17 is strongly expressed in ventral progenitor regions of the neural tube.**

681 (A-F) Expression of *GPR17*, Olig2 and Nkx2.2. *In situ* hybridisation analysis of *GPR17* on a section of
682 trunk neural tube was performed at HH stages 10 (A), 14 (C) and 24 (E), and the expression pattern was
683 compared with those of Olig2 (red) and Nkx2.2 (green), as determined by immunofluorescence (IF) at
684 equivalent stages (B,D,F). The ventral ends of the *GPR17* (E) and Nkx2.2 (F) expression are indicated
685 by arrowheads. Scale Bar in (A) for (A-F) = 100 μ m. (G) The *GPR17* expression profile was analysed
686 by RT-qPCR in the neural explants cultured in the absence or in the presence of Shh^L or Shh^H for
687 indicated time periods. (H) The *GPR17* expression is affected by Olig2 and FoxA2, but not by Znf488.
688 Neural explants electroporated with *control GFP* (lane 1), *Olig2* (lane 2), *FoxA2* (lane 3) or *Znf488*
689 (lane 4) were prepared and the expression of *GPR17* was analysed by qPCR after the 24 hour-culture.
690 (I) *GPR17* expression depends on Olig2. Neural explants electroporated with *control GFP* (lanes 1,2)
691 or *dn-Olig2* (lane 2) were cultured in the absence (lane 1) or in the presence (lanes 2,3) of Shh^L for 24
692 hours, and *GPR17* expression was analysed by RT-qPCR.

693

694 **Fig. 3. GPR17 is a negative regulator for the Shh signalling pathway.**

695 (A) Overexpression of GPR17 decreased the expression levels of *Ptch1* and *Gli1* following Pur
696 treatment. NIH3T3 cells transfected either with indicated plasmids were treated with Pur for 24 hours,
697 and expression of *Ptch1* and *Gli1* was analysed by RT-qPCR. (B) The processing of Gli3 was altered in
698 the *GPR17*-transfected cells. Control (lanes 1,3) or *GPR17* (lanes 2,4) expression plasmids were
699 transfected into the NIH3T3 cells and cells were cultured with 500 nM of Pur for 6 hours. The cell
700 lysates were analysed by western blotting. (C) The quantitative data of the total Gli3FL and Gli3R for
701 (B). (D) The cAMP level is upregulated by GPR17. NIH3T3 cells were transfected with control or
702 mouse *GPR17* expression plasmids. Intracellular cAMP was measured. (E) The CREB activity was
703 measured by a luciferase assay.

704

705 **Fig. 4. GPR17 negatively regulates the Shh signalling pathway and affects the cell identity of**
706 **neural progenitors.**

707 (A-L) The ventral identity was affected by MDL29951. The embryos were cultured with the New culture
708 system with the control solvent (DMSO; A,C,E,G,I,K) or with 100 μ M of MDL29951 (B,D,F,H,J,L)
709 and analysed the expression of Olig2 (A,B), Nkx2.2 (C,D), Pax7 (E,F), *Ptch1* (G,H), FoxA2 (I,J) and
710 *Shh* (K,L) by immunofluorescence (A-F,I,J) or by *in situ* hybridisation (G,H,K,L). Ventral ends of the
711 Pax7 expression is indicated by white arrowheads in (E,F). The Shh expression is indicated by black
712 arrowheads in (K,L). nc; notochord. (M) The dynamic Gli activity is affected in the neural explants
713 treated with Shh^H and MDL29951. Explants electroporated with *GBS-Luc* were treated with control
714 medium, Shh^H or Shh^H + MDL29951 for 6 or 24 hours. (N-T) Ventral identities are altered by treatment
715 with MDL29951, a specific agonist of GPR17. Explants were incubated for 24 hours with Shh^H in the
716 absence (N,P,R,T) or presence (O,Q,S,T) of 30 μ M MDL29951, and were stained with Olig2 (N,O,R,S)
717 and Nkx2.2 (P,Q,R,S) antibodies. Quantification in (T). (U) cAMP level is upregulated by the treatment
718 with MDL29951 in the intermediate neural explants. Explants were prepared and treated with control,
719 Shh^H or Shh^H + MDL29951 for 24 hours. Scale Bars in (A-L), and in (N) for (N-S) = 50 μ m.

720

721 **Fig. 5. Knockdown of GPR17 affects dorsal-ventral pattern formation of the neural tube.**

722 The neural tube was electroporated with *si-control* (A-A'',C-C'',E-E'',G-G'',I-I'') or *si-GPR17* (B-B'',D-
723 D'',F-F'',H-H'',J-J'') at HH stage 12 on the right side of the neural tube, and incubated for 48 hours until
724 the embryos reached HH stage 24. Sections of the neural tube were analysed with antibodies against
725 Olig2 (A-B''), Nkx2.2 (C-D''), FoxA2 (E-F''), Islet1 (G-H''), or Pax7 (I-J''). Scale bars in (A) for (A-
726 B''), (C) for (C-D''), (E) for (E-F''), (G) for (G-H''), and (I) for (I-J'') = 50 μ m. Expanded areas are
727 indicated by brackets and white arrowheads, and reduced areas are outlined arrowheads.

728

729 **Fig. 6. GPR17 controls temporal Gli activity.**

730 (A-H) Knockdown of *GPR17* induces more ventral identity. Intermediate neural explants electroporated
731 with *si-control* (A-D) or *si-GPR17* (E-H) were treated with Shh^L for 24 hours, and expression was
732 analysed with antibodies against Olig2 (A,B,E,F) or Nkx2.2 (C,D,G,H) and GFP (B,D,F,H). Scale Bar
733 in (A) for (A-H) = 50 μ m. (I) Quantitative data for (A-H). (J) Feedback of Gli activity is partially
734 perturbed by knocking-down of GPR17. Explants electroporated with *si-control* (blue line) or *si-GPR17*
735 (red line) together with *GBS-Luc* were incubated with Shh^L for indicated time points, and luciferase
736 activity was measured. (K) Prolonged expression of *Ptch1* in the intermediate neural explants treated
737 with Shh^L. *si-control*- (blue line) or *si-GPR17*- (red line) electroporated explants were treated with Shh^L
738 and the *Ptch1* mRNA level was analysed in the samples harvested every 12 hours. (L,M) Suppression
739 of *GPR17* expression changes the total amounts of the Gli3FL and Gli3R. Neural explants electroporated
740 with either *si-control* or *si-GPR17* were prepared and they were cultured for 6 (left panel) and 24 (right
741 panel) hours in the absence (lanes 1,2,5,6) or in the presence (lanes 3,4,7,8) of Shh and were analysed

742 by western blotting with the Gli3 antibody. (M) The total amounts of Gli3FL and Gli3R were quantified
743 from four independent experiments.

744

745 **Fig. 7. GPR17 is required for proper directed neural differentiation from mouse embryonic stem**
746 **cells.**

747 (A) GPR17 expression level is subtype-dependent. ES cells were differentiated according to the protocol
748 in Fig. S8A, and the expression levels of *GPR17* in each sample were analysed by RT-qPCR. (B-P)
749 Directed neural differentiation from ES cells. (B-E) MDL29951 has a dorsalising activity of the neural
750 fate. ES cells were differentiated according to the protocol (i) (Fig. S8A), which mainly yields pMN
751 cells. From day 3.5, DMSO (control; B,D) or 50 μ M of MDL29951 (C,E) was added into the medium,
752 in addition to RA and Shh as in the protocol. The cells were analysed with antibodies against Olig2
753 (B,D) and Pax6 (C,E). (F) Quantitative data for (B-E). (G-O) Effects of *si-RNAs* targeting *GPR17* for
754 the neural fate determination. ES cells transfected with *si-control* (G,J,M), *si-GPR17-1* (H,K,N) or *si-*
755 *GPR17-2* (I,L,O) were differentiated according to the protocol (i), and analysed with antibodies against
756 Olig2 (G-I) and Nkx2.2 (J-L). (P) Quantification of Olig2 and Nkx2.2 expressing cells over DAPI
757 positive cells. (Q) Expression levels of *Nkx2.2* and *Ptch1* were analysed by RT-qPCR. Scale bars in (B)
758 for (B-E), and in (G) for (G-O) = 50 μ m.

759

760 **Fig. 8. A working model for the negative regulation of the intracellular Shh signaling pathway.**

761 The binding of Shh (ligand) to Ptch (a membrane protein) abrogates its repressive effect on Smo, and
762 the conversion from the full-length forms (Gli2/3FL) to their repressor forms (Gli2/3R) is thereby
763 perturbed. Gli2/3FL are further modified to their active forms (Gli2/3A) and are translocated to the
764 nucleus where the target genes, including *Olig2* and *Ptch*, are induced. It has been shown that the
765 accumulation of *Ptch* transcript results in the perturbation of the Shh signal transduction. In addition, as
766 demonstrated in our study, *Olig2* induces the *GPR17* gene expression, and the upregulation of cAMP
767 encourages the accumulation of Gli2/3R. The positive and negative regulations are indicated by blue
768 and red lines, respectively. The transcriptional regulation is indicated by black lines.

769 **References**

770

771 Abrajano, J.J., Qureshi, I.A., Gokhan, S., Zheng, D., Bergman, A., Mehler, M.F., 2009. Differential
772 deployment of REST and CoREST promotes glial subtype specification and oligodendrocyte
773 lineage maturation. *PloS one* 4, e7665.

774 Balaskas, N., Ribeiro, A., Panovska, J., Dessaud, E., Sasai, N., Page, K.M., Briscoe, J., Ribes, V., 2012.
775 Gene regulatory logic for reading the Sonic Hedgehog signaling gradient in the vertebrate neural
776 tube. *Cell* 148, 273-284.

777 Belmokhtar, C.A., Hillion, J., Segal-Bendirdjian, E., 2001. Staurosporine induces apoptosis through
778 both caspase-dependent and caspase-independent mechanisms. *Oncogene* 20, 3354-3362.

779 Briscoe, J., 2006. Agonizing hedgehog. *Nature chemical biology* 2, 10-11.

780 Briscoe, J., Sussel, L., Serup, P., Hartigan-O'Connor, D., Jessell, T.M., Rubenstein, J.L., Ericson, J.,
781 1999. Homeobox gene *Nkx2.2* and specification of neuronal identity by graded Sonic hedgehog
782 signalling. *Nature* 398, 622-627.

783 Buccioni, M., Marucci, G., Dal Ben, D., Giacobbe, D., Lambertucci, C., Soverchia, L., Thomas, A.,
784 Volpini, R., Cristalli, G., 2011. Innovative functional cAMP assay for studying G protein-coupled
785 receptors: application to the pharmacological characterization of GPR17. *Purinergic signalling* 7,
786 463-468.

787 Ceruti, S., Villa, G., Genovese, T., Mazzon, E., Longhi, R., Rosa, P., Bramanti, P., Cuzzocrea, S.,
788 Abbracchio, M.P., 2009. The P2Y-like receptor GPR17 as a sensor of damage and a new potential
789 target in spinal cord injury. *Brain : a journal of neurology* 132, 2206-2218.

790 Chen, Y., Wu, H., Wang, S., Koito, H., Li, J., Ye, F., Hoang, J., Escobar, S.S., Gow, A., Arnett, H.A.,
791 Trapp, B.D., Karandikar, N.J., Hsieh, J., Lu, Q.R., 2009. The oligodendrocyte-specific G protein-
792 coupled receptor GPR17 is a cell-intrinsic timer of myelination. *Nature neuroscience* 12, 1398-
793 1406.

794 Ciana, P., Fumagalli, M., Trincavelli, M.L., Verderio, C., Rosa, P., Lecca, D., Ferrario, S., Parravicini,
795 C., Capra, V., Gelosa, P., Guerrini, U., Belcredito, S., Cimino, M., Sironi, L., Tremoli, E., Rovati,
796 G.E., Martini, C., Abbracchio, M.P., 2006. The orphan receptor GPR17 identified as a new dual
797 uracil nucleotides/cysteinyl-leukotrienes receptor. *The EMBO journal* 25, 4615-4627.

798 Cohen, M., Kicheva, A., Ribeiro, A., Blassberg, R., Page, K.M., Barnes, C.P., Briscoe, J., 2015. *Ptch1*
799 and *Gli* regulate *Shh* signalling dynamics via multiple mechanisms. *Nature communications* 6,
800 6709.

801 Delfino-Machin, M., Lunn, J.S., Breitkreuz, D.N., Akai, J., Storey, K.G., 2005. Specification and
802 maintenance of the spinal cord stem zone. *Development* 132, 4273-4283.

803 Dessaud, E., McMahon, A.P., Briscoe, J., 2008. Pattern formation in the vertebrate neural tube: a sonic
804 hedgehog morphogen-regulated transcriptional network. *Development* 135, 2489-2503.

805 Dessaud, E., Ribes, V., Balaskas, N., Yang, L.L., Pierani, A., Kicheva, A., Novitch, B.G., Briscoe, J.,
806 Sasai, N., 2010. Dynamic assignment and maintenance of positional identity in the ventral neural
807 tube by the morphogen sonic hedgehog. *PLoS biology* 8, e1000382.

808 Dessaud, E., Yang, L.L., Hill, K., Cox, B., Ulloa, F., Ribeiro, A., Mynett, A., Novitch, B.G., Briscoe,
809 J., 2007. Interpretation of the sonic hedgehog morphogen gradient by a temporal adaptation
810 mechanism. *Nature* 450, 717-720.

811 Epstein, D.J., Marti, E., Scott, M.P., McMahon, A.P., 1996. Antagonizing cAMP-dependent protein
812 kinase A in the dorsal CNS activates a conserved Sonic hedgehog signaling pathway. *Development*
813 122, 2885-2894.

814 Fumagalli, M., Lecca, D., Abbracchio, M.P., 2016. CNS remyelination as a novel reparative approach
815 to neurodegenerative diseases: The roles of purinergic signaling and the P2Y-like receptor GPR17.
816 *Neuropharmacology* 104, 82-93.

817 Hamburger, V., Hamilton, H.L., 1992. A series of normal stages in the development of the chick embryo.
818 1951. *Developmental dynamics : an official publication of the American Association of Anatomists*
819 195, 231-272.

820 Hammerschmidt, M., Bitgood, M.J., McMahon, A.P., 1996. Protein kinase A is a common negative
821 regulator of Hedgehog signaling in the vertebrate embryo. *Genes & development* 10, 647-658.

822 Hennen, S., Wang, H., Peters, L., Merten, N., Simon, K., Spinrath, A., Blattermann, S., Akkari, R.,
823 Schrage, R., Schroder, R., Schulz, D., Vermeiren, C., Zimmermann, K., Kehraus, S., Drewke, C.,
824 Pfeifer, A., Konig, G.M., Mohr, K., Gillard, M., Muller, C.E., Lu, Q.R., Gomeza, J., Kostenis, E.,

2013. Decoding signaling and function of the orphan G protein-coupled receptor GPR17 with a small-molecule agonist. *Science signaling* 6, ra93.

Heppenstall, P.A., Fleetwood-Walker, S.M., 1997. The glycine site of the NMDA receptor contributes to neurokinin1 receptor agonist facilitation of NMDA receptor agonist-evoked activity in rat dorsal horn neurons. *Brain research* 744, 235-245.

Holz, A., Kollmus, H., Ryge, J., Niederkofler, V., Dias, J., Ericson, J., Stoeckli, E.T., Kiehn, O., Arnold, H.H., 2010. The transcription factors Nkx2.2 and Nkx2.9 play a novel role in floor plate development and commissural axon guidance. *Development* 137, 4249-4260.

Humke, E.W., Dorn, K.V., Milenkovic, L., Scott, M.P., Rohatgi, R., 2010. The output of Hedgehog signaling is controlled by the dynamic association between Suppressor of Fused and the Gli proteins. *Genes & development* 24, 670-682.

Jansen, M., Dannhardt, G., 2003. Antagonists and agonists at the glycine site of the NMDA receptor for therapeutic interventions. *European journal of medicinal chemistry* 38, 661-670.

Jenie, R.I., Nishimura, M., Fujino, M., Nakaya, M., Mizuno, N., Tago, K., Kurose, H., Itoh, H., 2013. Increased ubiquitination and the crosstalk of G protein signaling in cardiac myocytes: involvement of Ric-8B in Gs suppression by Gq signal. *Genes to cells : devoted to molecular & cellular mechanisms* 18, 1095-1106.

Kamiya, D., Banno, S., Sasai, N., Ohgushi, M., Inomata, H., Watanabe, K., Kawada, M., Yakura, R., Kiyonari, H., Nakao, K., Jakt, L.M., Nishikawa, S., Sasai, Y., 2011. Intrinsic transition of embryonic stem-cell differentiation into neural progenitors. *Nature* 470, 503-509.

Kutejova, E., Sasai, N., Shah, A., Gouti, M., Briscoe, J., 2016. Neural Progenitors Adopt Specific Identities by Directly Repressing All Alternative Progenitor Transcriptional Programs. *Developmental cell* 36, 639-653.

Lander, A.D., 2011. Pattern, growth, and control. *Cell* 144, 955-969.

Le Dreau, G., Marti, E., 2012. Dorsal-ventral patterning of the neural tube: a tale of three signals. *Developmental neurobiology* 72, 1471-1481.

Lecca, D., Trincavelli, M.L., Gelosa, P., Sironi, L., Ciana, P., Fumagalli, M., Villa, G., Verderio, C., Grumelli, C., Guerrini, U., Tremoli, E., Rosa, P., Cuboni, S., Martini, C., Buffo, A., Cimino, M., Abbracchio, M.P., 2008. The recently identified P2Y-like receptor GPR17 is a sensor of brain damage and a new target for brain repair. *PloS one* 3, e3579.

Litingtung, Y., Chiang, C., 2000. Specification of ventral neuron types is mediated by an antagonistic interaction between Shh and Gli3. *Nature neuroscience* 3, 979-985.

Lu, C., Dong, L., Zhou, H., Li, Q., Huang, G., Bai, S.J., Liao, L., 2018. G-Protein-Coupled Receptor Gpr17 Regulates Oligodendrocyte Differentiation in Response to Lysolecithin-Induced Demyelination. *Scientific reports* 8, 4502.

Lu, Q.R., Yuk, D., Alberta, J.A., Zhu, Z., Pawlitzky, I., Chan, J., McMahon, A.P., Stiles, C.D., Rowitch, D.H., 2000. Sonic hedgehog--regulated oligodendrocyte lineage genes encoding bHLH proteins in the mammalian central nervous system. *Neuron* 25, 317-329.

Megason, S.G., McMahon, A.P., 2002. A mitogen gradient of dorsal midline Wnts organizes growth in the CNS. *Development* 129, 2087-2098.

Merten, N., Fischer, J., Simon, K., Zhang, L., Schroder, R., Peters, L., Letombe, A.G., Hennen, S., Schrage, R., Bodefeld, T., Vermeiren, C., Gillard, M., Mohr, K., Lu, Q.R., Brustle, O., Gomeza, J., Kostenis, E., 2018. Repurposing HAMI3379 to Block GPR17 and Promote Rodent and Human Oligodendrocyte Differentiation. *Cell chemical biology* 25, 775-786 e775.

Moore, B.S., Stepanchick, A.N., Tewson, P.H., Hartle, C.M., Zhang, J., Quinn, A.M., Hughes, T.E., Mirshahi, T., 2016. Cilia have high cAMP levels that are inhibited by Sonic Hedgehog-regulated calcium dynamics. *Proceedings of the National Academy of Sciences of the United States of America* 113, 13069-13074.

Mukhopadhyay, S., Wen, X., Ratti, N., Loktev, A., Rangell, L., Scales, S.J., Jackson, P.K., 2013. The ciliary G-protein-coupled receptor Gpr161 negatively regulates the Sonic hedgehog pathway via cAMP signaling. *Cell* 152, 210-223.

Niewiadowski, P., Kong, J.H., Ahrends, R., Ma, Y., Humke, E.W., Khan, S., Teruel, M.N., Novitch, B.G., Rohatgi, R., 2014. Gli protein activity is controlled by multisite phosphorylation in vertebrate Hedgehog signaling. *Cell reports* 6, 168-181.

Oh, S., Huang, X., Chiang, C., 2005. Specific requirements of sonic hedgehog signaling during oligodendrocyte development. *Developmental dynamics : an official publication of the American Association of Anatomists* 234, 489-496.

882 Ou, Z., Sun, Y., Lin, L., You, N., Liu, X., Li, H., Ma, Y., Cao, L., Han, Y., Liu, M., Deng, Y., Yao, L.,
883 Lu, Q.R., Chen, Y., 2016. Olig2-Targeted G-Protein-Coupled Receptor Gpr17 Regulates
884 Oligodendrocyte Survival in Response to Lysolecithin-Induced Demyelination. *The Journal of*
885 *neuroscience : the official journal of the Society for Neuroscience* 36, 10560-10573.

886 Pan, Y., Bai, C.B., Joyner, A.L., Wang, B., 2006. Sonic hedgehog signaling regulates Gli2
887 transcriptional activity by suppressing its processing and degradation. *Molecular and cellular*
888 *biology* 26, 3365-3377.

889 Pan, Y., Wang, C., Wang, B., 2009. Phosphorylation of Gli2 by protein kinase A is required for Gli2
890 processing and degradation and the Sonic Hedgehog-regulated mouse development.
891 *Developmental biology* 326, 177-189.

892 Parravicini, C., Abbracchio, M.P., Fantucci, P., Ranghino, G., 2010. Forced unbinding of GPR17
893 ligands from wild type and R255I mutant receptor models through a computational approach. *BMC*
894 *structural biology* 10, 8.

895 Parravicini, C., Ranghino, G., Abbracchio, M.P., Fantucci, P., 2008. GPR17: molecular modeling and
896 dynamics studies of the 3-D structure and purinergic ligand binding features in comparison with
897 P2Y receptors. *BMC bioinformatics* 9, 263.

898 Perrimon, N., Pitsouli, C., Shilo, B.Z., 2012. Signaling mechanisms controlling cell fate and embryonic
899 patterning. *Cold Spring Harbor perspectives in biology* 4, a005975.

900 Psychoyos, D., Finnell, R., 2008. Method for Culture of Early Chick Embryos ex vivo (New Culture).
901 *Journal of visualized experiments : JoVE*.

902 Pusapati, G.V., Kong, J.H., Patel, B.B., Gouti, M., Sagner, A., Sircar, R., Luchetti, G., Ingham, P.W.,
903 Briscoe, J., Rohatgi, R., 2018. G protein-coupled receptors control the sensitivity of cells to the
904 morphogen Sonic Hedgehog. *Science signaling* 11.

905 Rehimi, R., Nikolic, M., Cruz-Molina, S., Tebartz, C., Frommolt, P., Mahabir, E., Clement-Ziza, M.,
906 Rada-Iglesias, A., 2016. Epigenomics-Based Identification of Major Cell Identity Regulators
907 within Heterogeneous Cell Populations. *Cell reports* 17, 3062-3076.

908 Ribes, V., Briscoe, J., 2009. Establishing and interpreting graded Sonic Hedgehog signaling during
909 vertebrate neural tube patterning: the role of negative feedback. *Cold Spring Harbor perspectives*
910 *in biology* 1, a002014.

911 Rosenbaum, D.M., Rasmussen, S.G., Kobilka, B.K., 2009. The structure and function of G-protein-
912 coupled receptors. *Nature* 459, 356-363.

913 Sasai, N., Briscoe, J., 2012. Primary cilia and graded Sonic Hedgehog signaling. *Wiley interdisciplinary*
914 *reviews. Developmental biology* 1, 753-772.

915 Sasai, N., Kutejova, E., Briscoe, J., 2014. Integration of signals along orthogonal axes of the vertebrate
916 neural tube controls progenitor competence and increases cell diversity. *PLoS biology* 12,
917 e1001907.

918 Sasaki, H., Nishizaki, Y., Hui, C., Nakafuku, M., Kondoh, H., 1999. Regulation of Gli2 and Gli3
919 activities by an amino-terminal repression domain: implication of Gli2 and Gli3 as primary
920 mediators of Shh signaling. *Development* 126, 3915-3924.

921 Simon, K., Hennen, S., Merten, N., Blattermann, S., Gillard, M., Kostenis, E., Gomeza, J., 2016. The
922 Orphan G Protein-coupled Receptor GPR17 Negatively Regulates Oligodendrocyte Differentiation
923 via Galphai/o and Its Downstream Effector Molecules. *The Journal of biological chemistry* 291,
924 705-718.

925 Singh, J., Wen, X., Scales, S.J., 2015. The Orphan G Protein-coupled Receptor Gpr175 (Tpra40)
926 Enhances Hedgehog Signaling by Modulating cAMP Levels. *The Journal of biological chemistry*
927 290, 29663-29675.

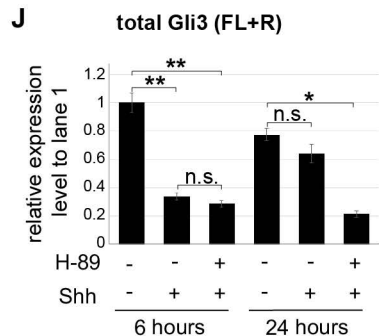
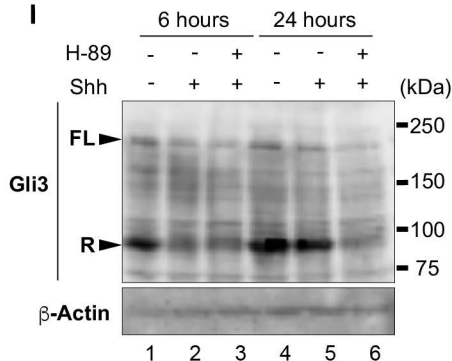
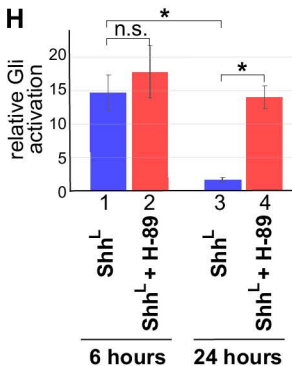
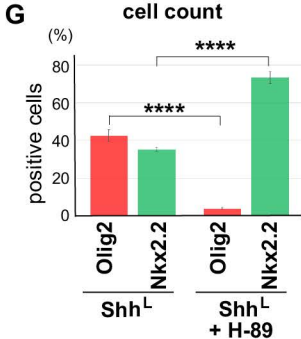
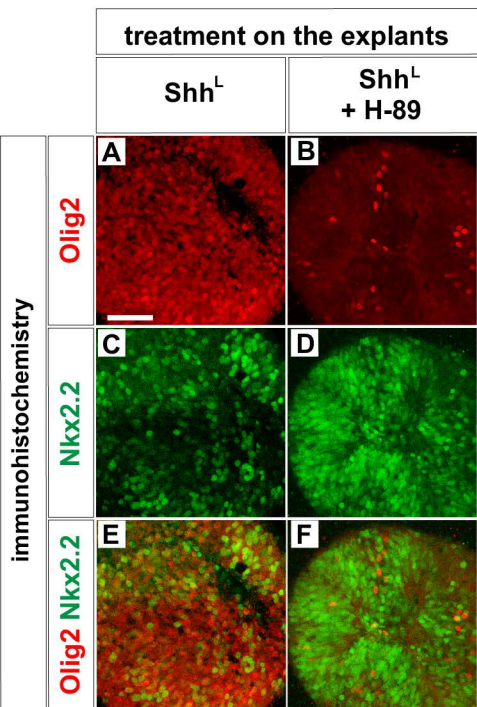
928 Stamatakis, D., Ulloa, F., Tsoni, S.V., Mynett, A., Briscoe, J., 2005. A gradient of Gli activity mediates
929 graded Sonic Hedgehog signaling in the neural tube. *Genes & development* 19, 626-641.

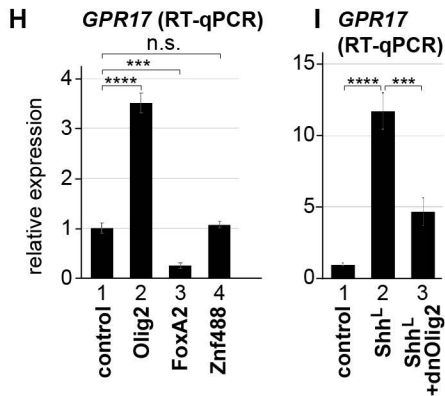
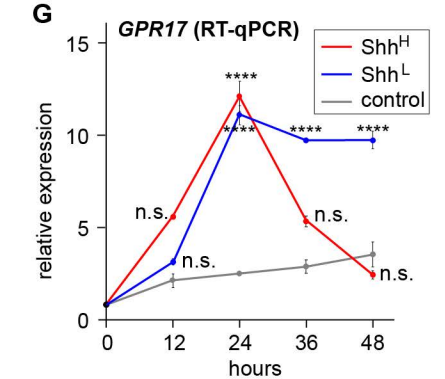
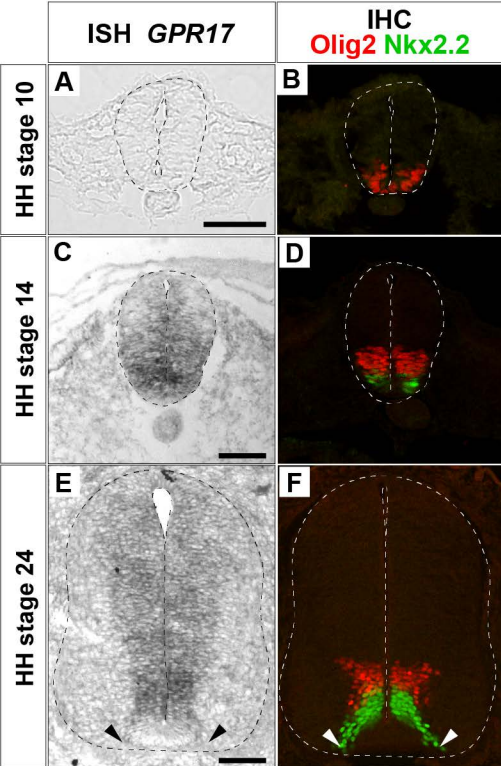
930 Tempe, D., Casas, M., Karaz, S., Blanchet-Tournier, M.F., Concordet, J.P., 2006. Multisite protein
931 kinase A and glycogen synthase kinase 3beta phosphorylation leads to Gli3 ubiquitination by
932 SCFbetaTrCP. *Molecular and cellular biology* 26, 4316-4326.

933 Tuson, M., He, M., Anderson, K.V., 2011. Protein kinase A acts at the basal body of the primary cilium
934 to prevent Gli2 activation and ventralization of the mouse neural tube. *Development* 138, 4921-
935 4930.

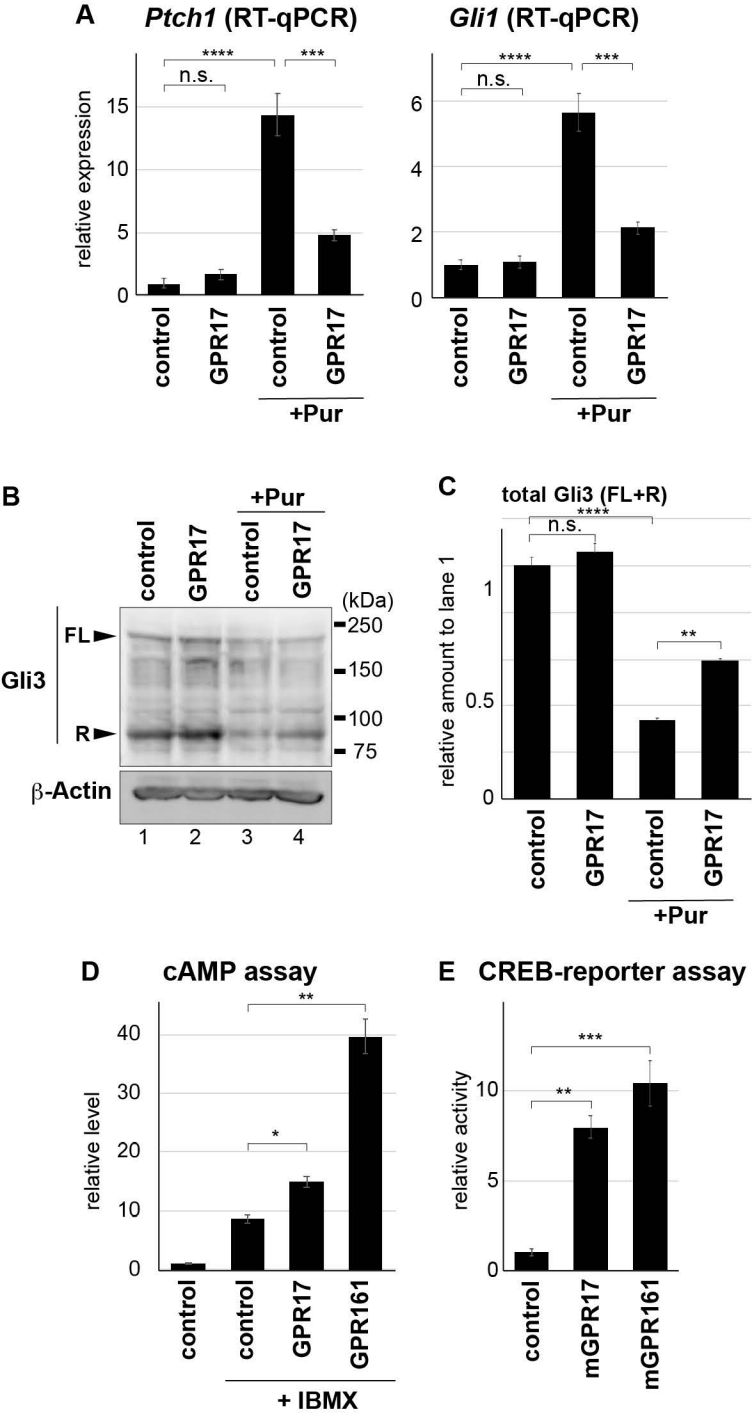
936 Vuolo, L., Herrera, A., Torroba, B., Menendez, A., Pons, S., 2015. Ciliary adenylyl cyclases control the
937 Hedgehog pathway. *Journal of cell science* 128, 2928-2937.

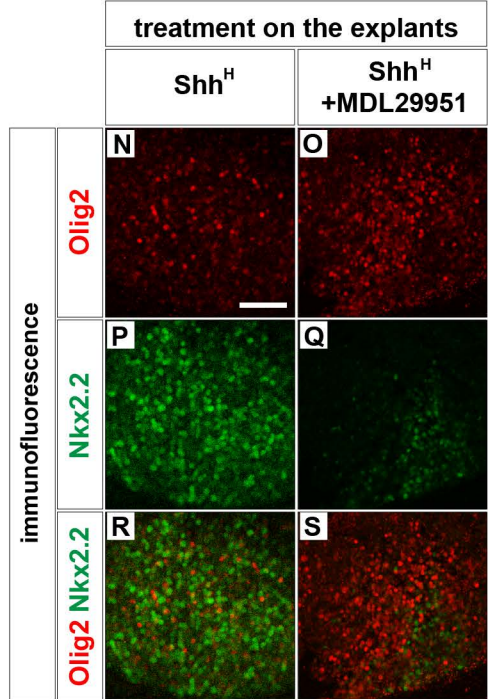
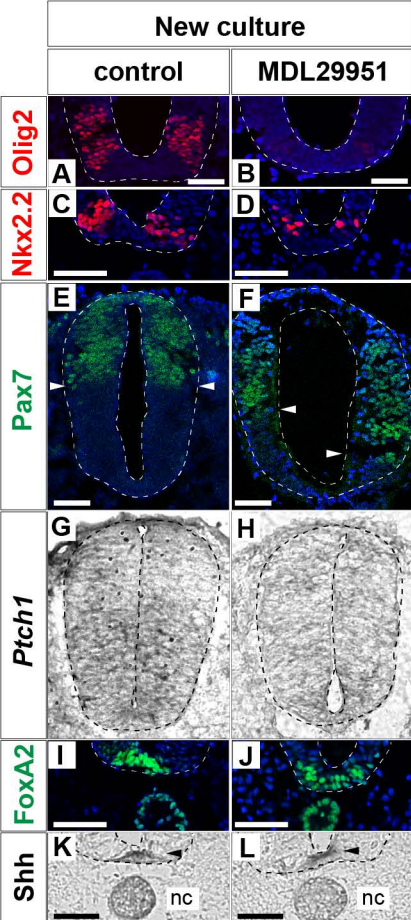
938 Wang, B., Fallon, J.F., Beachy, P.A., 2000. Hedgehog-regulated processing of Gli3 produces an
939 anterior/posterior repressor gradient in the developing vertebrate limb. *Cell* 100, 423-434.
940 Wang, B., Li, Y., 2006. Evidence for the direct involvement of β TrCP in Gli3 protein processing.
941 *Proceedings of the National Academy of Sciences of the United States of America* 103, 33-38.
942 Wang, S.Z., Dulin, J., Wu, H., Hurlock, E., Lee, S.E., Jansson, K., Lu, Q.R., 2006. An oligodendrocyte-
943 specific zinc-finger transcription regulator cooperates with Olig2 to promote oligodendrocyte
944 differentiation. *Development* 133, 3389-3398.
945 Wolpert, L., 1969. Positional information and the spatial pattern of cellular differentiation. *Journal of*
946 *theoretical biology* 25, 1-47.
947 Ying, Q.L., Stavridis, M., Griffiths, D., Li, M., Smith, A., 2003. Conversion of embryonic stem cells
948 into neuroectodermal precursors in adherent monoculture. *Nature biotechnology* 21, 183-186.
949 Zhou, Q., Anderson, D.J., 2002. The bHLH transcription factors OLIG2 and OLIG1 couple neuronal
950 and glial subtype specification. *Cell* 109, 61-73.
951 Zhou, Q., Choi, G., Anderson, D.J., 2001. The bHLH transcription factor Olig2 promotes
952 oligodendrocyte differentiation in collaboration with Nkx2.2. *Neuron* 31, 791-807.
953
954



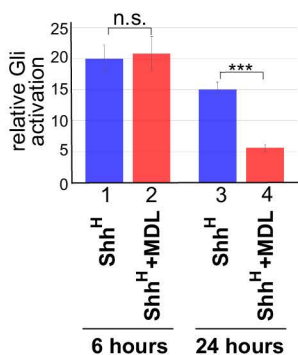


Yatsuzuka et al., Figure 2

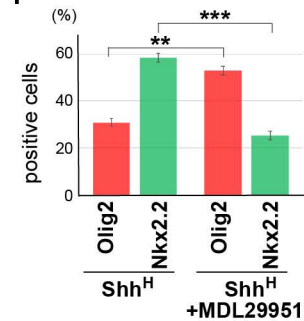




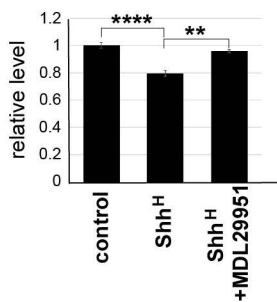
M Gli activity

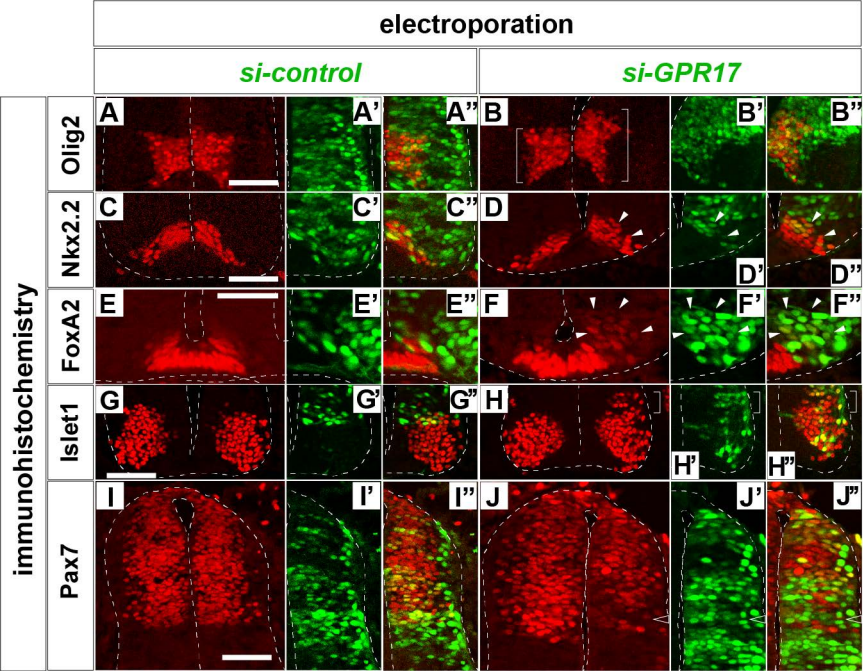


T cell count

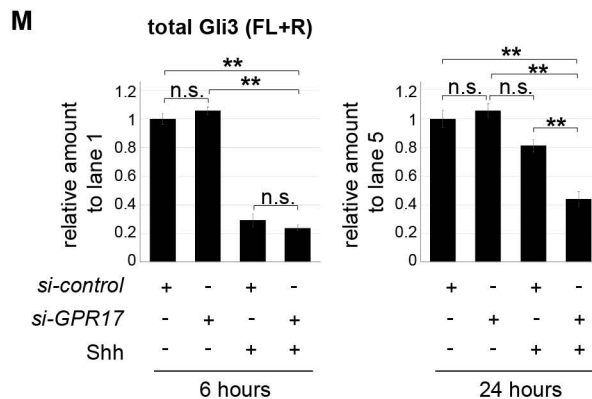
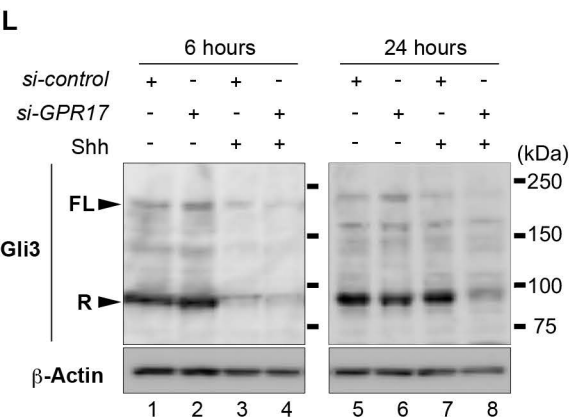
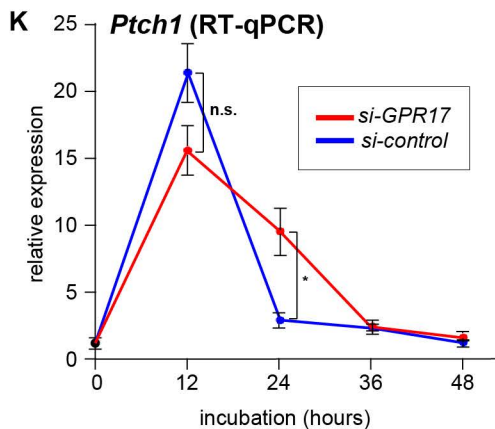
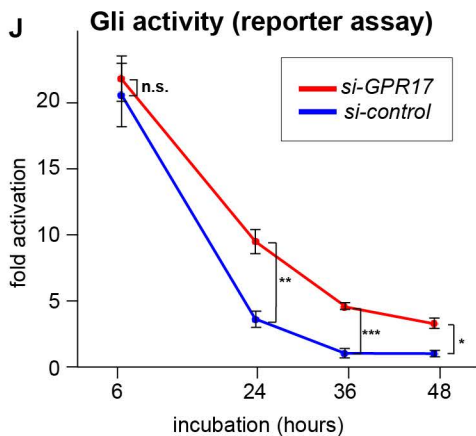
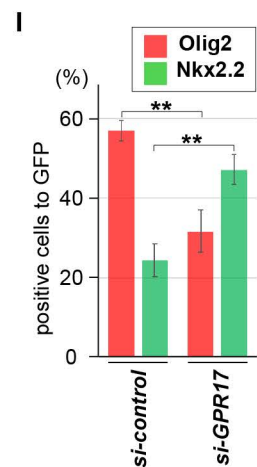
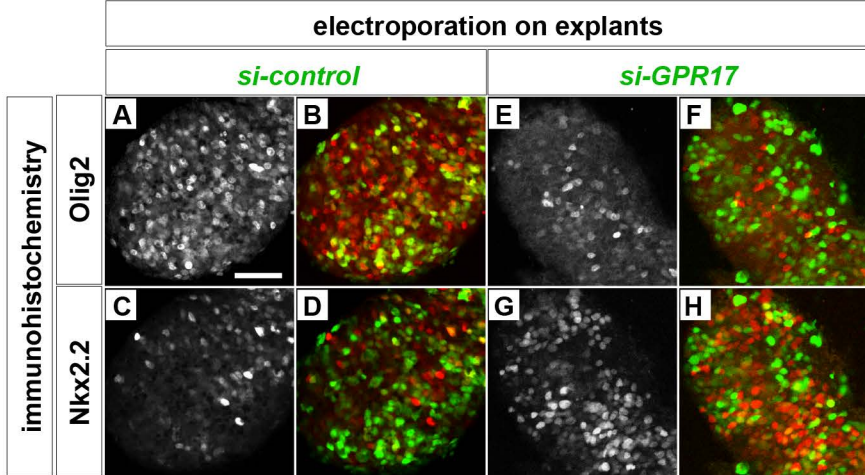


U cAMP assay

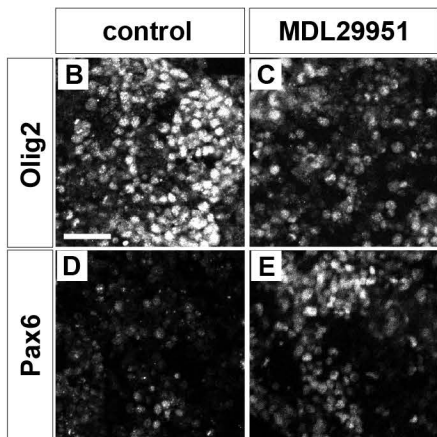
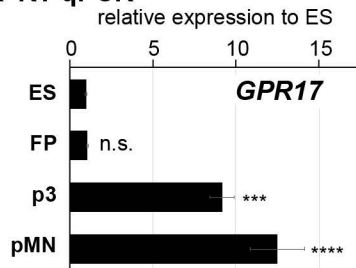




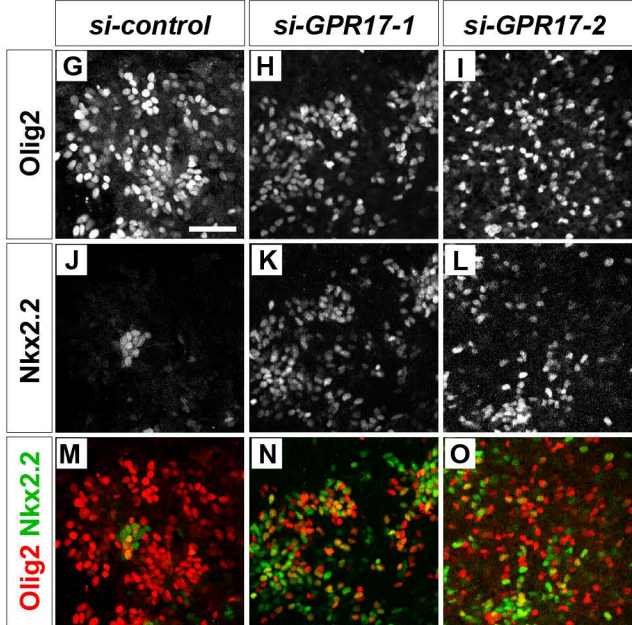
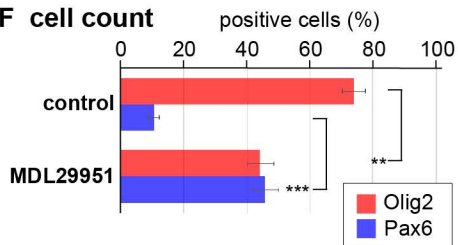
Yatsuzuka et al., Figure 5



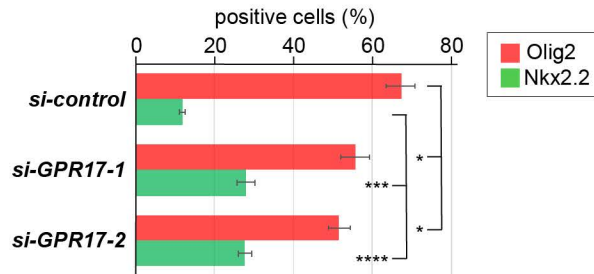
A RT-qPCR



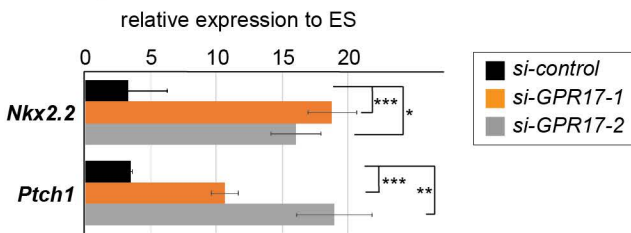
F cell count

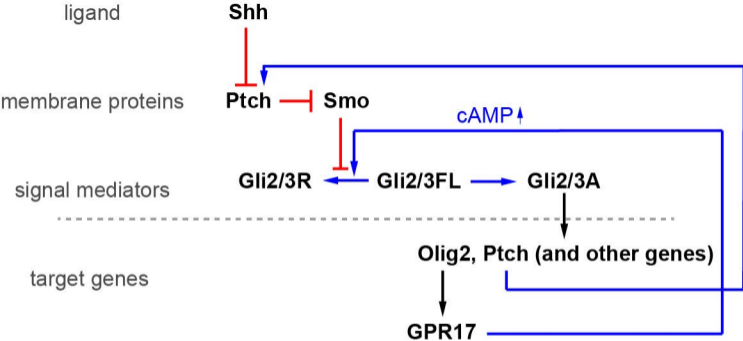


P cell count



Q RT-qPCR





Yatsuzuka et al., Figure 8